Review of solidification and melting performance of phase change materials in the presence of magnetic field, rotation, tilt angle, and vibration

Farhan Lafta Rashid [1], Alireza Rahbari [2], Raed Khalid Ibrahem[3], Pouyan Talebizadehsardari [4,*], Ali basem [5], Amr Kaood [6], Hayder I. Mohammed [7], Mohammed H Abbas [8], Mudhar A. Al-Obaidi [9,10]

[1] Petroleum Engineering Department, College of Engineering, University of Kerbala, Karbala 56001, Iraq
[2] School of Engineering, the Australian National University, Canberra ACT 2601, Australia
[3] Department of Medical Instrumentation Engineering Techniques, Al-Farahidi University, Baghdad 10015, Iraq
[4] Centre for Sustainable Energy use in Food Chains, Institute of Energy Futures, Brunel University London, Kingston Lane, Uxbridge, Middlesex UB8 3PH, UK
[5] Air Conditioning Engineering Department, Faculty of Engineering, Warith Al-Anbiyaa University, Iraq
[6] Mechanical Engineering Department, Faculty of Engineering, Fayoum University, El-Fayoum, 63514, Egypt
[7] Department of Physics, College of Education, University of Garmian, Kurdistan, Kalar 46021, Iraq
[8] Medical Physics Department, Al-Mustaqbal University College, Babylon, Iraq.
[9] Middle Technical University, Technical Institute of Baquba, Baquba, Diyala 32001, Iraq
[10] Middle Technical University, Technical Instructor Training Institute, Baghdad 10074, Iraq

*Corresponding author, E-mail address: pouyan.talebizadehsardari@brunel.ac.uk

Abstract

Due to the poor thermal conductivity of phase change materials (PCMs), the operation of Latent heat thermal energy storage (LHTES) is restricted by the limited heat exchange rate between PCMs and heat sources or sinks. The current review discusses the effects of magnetic field, rotation, tilt angle, and vibration on the discharging and charging heat performance of PCMs and nano-enhanced PCMs (NEPCMs) which are encapsulated in various container geometries and orientations based on melting and solidification standpoints. From this review, it is concluded that the orientation and design of the heat exchanger has a significant effect on the melting/solidification performance. The melting and solidification performance have been improved by increasing the magnetic number and decreasing the Hartmann number. Moreover, rotating cavity in a counter direction of buoyancy flow has improved the melting rate/time. The optimum tilting angle varies depending on the thickness of PCM layers. In terms of the vibration effect, frequency and amplitude/frequency are found to have an important role at low and high discharge rates, respectively. Following a comprehensive review, a few suggestions are provided as future research topic in this field.

***Keywords*:** Phase change materials; Latent heat thermal energy storage, Magnetic field; Rotation; Tilt angle; Vibration.

Contents

1. Introduction

To mitigate the solar fluctuations and ensure an uninterrupted supply of renewable energy, electrochemical storage systems (ESS) and thermal energy storage (TES) systems enable the storage of surplus energy for the use in downstream applications during high-demand periods. There are three main methods to store thermal energy including sensible heat storage, latent heat storage, and thermal storage—among which latent heat TES (LHTES) using phase change materials (PCMs) provide a higher storage density at relatively smaller size and lower temperature difference between releasing and storing processes [1,2].

PCMs have been widely used in the residential structures, building envelopes, and concentrated solar thermal systems [3-5]. They are arranged in sphere, rods, solid cylinders, solid flat plates, and other enclosure types [6-10]. PCMs are classified as organics (paraffins and non-paraffins), inorganics (salt hydrates and metallics), and eutectics of inorganic and organic compounds (organic-organic, inorganic-inorganic, and inorganic-organic) [11]. Inorganic PCMs have high latent heat values and high thermal conductivity. However, the main challenges with inorganic PCMs are corrosion, improper re-solidification, instability, which result in phase decomposition, and sub-cooling. Organic PCMs are more chemically stable than inorganic PCMs, but at the expense of inferior heat transfer characteristics, higher volume change, and flammability. Eutectics, the final type of PCM, have a high volumetric thermal storage density, high thermal conductivity, and a high latent heat of fusion per unit volume, although they are relatively expensive and heavy [12].

In order to improve the heat transfer properties of PCMs, several heat transfer enhancement techniques have been suggested in the literature. Active techniques rely on an external energy source such as electrohydrodynamic (EHD), magnetohydrodynamics (MHD), surface vibration, and mechanical motion to enhance the heat transfer rate [13, 14]. On the other hand, passive techniques do not require external forces and are primarily concerned with (i) surface modification through adding fins with various geometries (such as longitudinal fins [11, 15], circular fins [16-20], angled fins [21, 22], twisted fins [23], and tree-like branching and rectangular fins [24]), (ii) employing nanoparticles into the base fluid [25-27] (such as CuO [28, 29], copper [30], aluminum oxide and silver [31], or aluminum matrix [32]), (iii) using porous materials [33-35], (iv) changing the channel arrangement of the heat transfer fluid (HTF) [36-38], and (v) changing the configuration of the systems [5, 39-42]. Compound method is referred to a combination of active and passive techniques to improve the heat transfer.

During recent years, there has been a growing tendency towards investigating the heat transfer enhancement between PCMs and heat sources for various industrial applications. In this regard, several review papers have been published considering the employment of different enhancement methods including the metal foam [43], nanofluid [44], extended surfaces [45], and hybrid approaches [11]. To the best of authors' knowledge, there is a lack of a detailed review to highlight the effects of magnetic field, rotation, tilt angle, and vibration on the thermal storage performance of PCMs and nano-enhanced PCMs (NEPCMs) at variable container geometries. There are no holistic evaluations of the many findings from various experimental and numerical investigations regarding the effect of these techniques in the literature. The above-mentioned approaches have been deployed in a wide range of applications such as air conditioning and refrigeration industries, heat exchanger, compact electronics, and medical field [46]. Due to its significant contribution to improve the heat transfer [13, 14], this review aims at evaluating the emerging trends in enhancing the heat transfer rate and shortening the melting/solidification time of PCMs/NEPCMs for several industrial applications. This is followed by concluding remarks complemented by key topics for future work.

2. Methodology

This paper presents a comprehensive review on the effect of magnetic field, rotation, tilting angle, and vibration on the performance of PCM-based storage systems. A wide range of PCM/NEPCM container geometries including rectangular, cylindrical, square, annulus, and shell-and-tube is considered from melting and solidification perspectives. The advantages and disadvantages of each parameter are discussed in detail. The literature review is based on the papers selected from diverse academic databases and publishers including ELSEVIER, MDPI, ScienceDirect, Springer, and international conferences.

The first section of this review is dedicated to magnetic field role in various containers of PCMs/NEPCMs. Different important concepts including Lorentze force, Hatman number, Reynolds number, nanoparticles effect, fins/metal foam addition, uniformity and types of the magnetic field are discussed in this section. The second section focused on the role of rotation on the melting and solidification performance of PCMs/NEPCMs. The objective of this section is to gain further understanding on how rotational speed/mode and container geometries can influence the phase change process. The next section presents a review on whether tilting angle of either heating surface or phase change container enhances or deteriorates the PCM melting/solidification processes. The synergy between this parameter and fin/nanoparticle addition has been evaluated to check how the conclusions might change in the presence of these parameters. The last section is devoted to the vibration effect considering PCM container configurations, and the frequency/amplitude of the vibration. At the beginning of each section, there is a table summarising the type of study either numerical or experimental, studied parameters, and key take-away findings of each paper. This is followed by a detailed discussion in the subsequent subsections. The last section summarises the key findings of this review followed by some recommendations for future work.

This paper provides a well-organized review that includes the definition, description, configuration, examined parameters, and most important conclusions of the selected articles. The emerging trends in renewable energy uptake, more specifically solar energy, for various industrial applications require a detailed review, essentially pointing toward techniques to overcome the challenges associated with charging/discharging response of LHTES technologies.

3. Effect of magnetic field

Magnetic-field is a method to control the convective heat transfer inside an enclosure. Table 1 lists the geometrical, operating conditions, and key take-away findings of recent studies addressing the role magnetic field on the melting/solidification procedures of PCMs/NEPCMs encapsulated inside an enclosure with different geometries. The citation list [8, 47–65] focuses on this importance in different geometries as summarized in the following subsections.

Table 1. A summary of studies on magnetic field effect on the melting/solidification procedures of PCMs/NEPCMs inside an enclosure with different geometries

Authors (year)	**Configuration**	**Type of study**	**Studied parameters**	**Highlighted results/findings**
Sheikholeslami and Mahian (2019) [8]	Porous annulus containing NEPCM	Numerical	Effect of Lorentz force, NEPCM concentration, and Rayleigh number on the solidification process	23.5% reduction in the solidification time by increasing the Hartmann number from 0 to 10. 14% decrease in the solidification time can be accomplished by adding nanoparticle up to 4% concentration.
Lei et al. (2015) [47]	Rectangular cavity containing dispersed carbon nanomaterial and sodium dodecyl benzene sulfonate (SDBS) in paraffin	Experimental	Effect of magnetic field on the solidification process	Homogeneous distribution of the particles in the solid area as a result of induced electromagnetic field.
Laouer et al. (2021) [48]	Copper-water NEPCM inside a rectangular cavity enclosure	Numerical	Effect of Hartmann number, nanoparticle volume fraction, and Rayleigh number on the melting of Cu-Ice	Decreased melting time by 10% at high Rayleigh number of 10^5 in the absence of magnetic field. Shortening the charging time at low Rayleigh number, while extending at high Rayleigh number with the addition of nanoparticle and in the presence of magnetic field.
Fan et al. (2021) [49]	Scattered magnetic particles with rotating magnetic field and PCM inside an inner layer of a glass casting cylinder	Experimental	Effect of particle fraction and rotational speed on the melting process	Rotational speed of 20 $r.min^{-1}$ with 1.0 wt.% particle fraction shortened the melting time by 22.9%. Vertical solid-liquid interface as a result of induced forced convection by the magnetic field.
Farahani et al. (2022) [50]	Employing fines with different shapes in a 3D cylindrical enclosure containing PCM	Numerical	Effect of fin shapes, non-uniform magnetic field and fin materials on the melting process	Improvement in the charging rate by 31.8% and 37.87% for continuous spiral fins and rectangular fins. Non-uniform magnetic field as a dominant parameter in accelerating the melting rate by 78% in case of spiral fins. 3% enhancement in the melting process through fabricating the fins from copper rather than aluminum.
Farahani et al. (2022) [51]	Nanoparticles embedded PCM in a 3D cylindrical enclosure with novel fin shapes	Numerical	Effect of non-uniform magnetic field, fin shape, and nanoparticle volume fraction on the melting process	Wide range of improvement in the melting process (i.e. 2–40%) depending of the fin shape. 1.5–2.5% increase in the melting fraction as a result of an increase in the nanoparticle volume fraction from 2.5 to 5%. Enhancement in the charging process when the strength of the magnetic field increased in the range of 16–57%.
Saha (2022) [52]	Gallium PCM in a semi-circular container with the heated circumferential wall	Numerical	Effect of magnetic field strength/direction, Rayleigh number, gravity conditions, and Marangoni number on the melting and solidification processes	Marginal effect of magnetic field direction on the charging/discharging performance. Prolonged duration of the melting time at higher Hartmann numbers. Shortened melting time under microgravity condition due to the thermos-capillary convection with/without the magnetic field.

Selimefendigil and Öztop (2022) [53]	Convection of hybrid nanofluid in a PCM-filled cylinder	Numerical	Effect of bifurcation location, Hartmann number, Reynolds number, and nanoparticle concentration on the melting and solidification processes	Decrease in the phase change time by 73% and 26% for bifurcating and flat channels at higher Reynolds number. Opposite behavior of phase-change dynamics for bifurcation and flat channels when magnetic field strength varied.
Kohyani et al. (2017) [54]	Cyclohexane–copper nano-PCM in a square porous cavity	Numerical	Effect of porosity, Hartmann number, solid volume fraction, and Rayleigh number (Ra) on the melting process	Reducing the melting time in the presence of the magnetic field. Intensified melting rate by increasing the Rayleigh number. Porosity as a more dominant factor compared to solid volume fraction.
Ghalambaz et al. (2019) [55]	Non-Newtonian behavior of magneto- and ferro-hydrodynamic PCM in a filled 2D square enclosure	Numerical	Effect of Rayleigh number, Hartmann number, Power-law index, and magnetic parameter on the melting front, Nusselt number, and normalized melt volume fraction (NMVF)	Slowing down the melting process by increasing the Hartmann number. Intensification in the Nusselt number by increasing the power index and magnetic parameter, and reducing the Hartmann number. Enhancement and reduction in the NMVF by increasing magnetic parameter and Hartmann number.
Mehryan et al. (2019) [56]	PCM-filled 2D square cavity subjected to two magnetic fields	Numerical	Effect of non-uniform magnetic source with different strength on the melting process	Intensity of the magnetic fields as the dominant factor on the progress of the melting front. Reduction in the melting front by an increase in the Hartmann number.
Kumar et al. (2022) [57]	Paraffin PCM and copper nanoparticles in a 2D square cavity	Numerical	Effect of heated wall orientation and nanoparticle volume fraction on the melting process under uniform magnetic field on the melting process	Maximum melting rate and energy storage capacity at a 2% and 0.5% nanoparticle concentration. Reduction in the stored energy capacity by 9% under different orientations of the cavity due to an increase in the magnetic field intensity.
Dibavar et al. (2018) [58]	NEPCM inside an annulus enclosure	Numerical	Effect of non-uniform magnetic on the melting and solidification processes	Reducing the time required for charging and discharging processes by up to 39.91% and 14.29% for non-electrical conductive magnetic nanofluid. Accelerated melting/solidification by increasing the magnetic number, while deteriorated melting/solidification by increasing the Hartmann number in case of electrical conductive ferrofluid.
Sheikholeslami (2018) [59]	CuO nanoparticles NEPCM in a porous TES curved enclosure in the presence of	Numerical	Effect of Hartmann number, volume fraction of nanofluid and Rayleigh number on the solidification process	Promoting the solidification performance by applying Lorentz forces. Reverse relationship between the solidification time with the volume fraction of nanofluid and Hartmann number.
Ghalambaz et al. (2019) [60]	Analysing the transmission of heat via moving mesh method in electrically conductive PCM inside a cavity enclosure	Numerical	Effect of Hartmann number and the location of non-uniform magnetic fields on the melting process	Significant effect of magnetic field at later stages of the melting process (Fourier number, Fo, greater than 1.15). Reduced Fo from 10.4 to 9.0 by changing the location of magnetic source from the bottom to middle of the cavity.
Shi et al. (2020) [61]	Paraffin type A16 with Fe_3O_4 nanoparticles in a 3D shell and multi-tube TES system	Numerical	Effect of quadrupole magnet field on the melting and solidification processes,	80.02% and 53.19% improvement in the charging and discharging time for the magnetic field with 50 mT intensity. Longer solidification time compared to the charging time with and without magnetic field.

				Improving the cyclic processes through reducing the difference between charging and discharging time in the presence of the magnetic field.
Selimefendigil and Öztop (2020) [62]	Artificial neural network (ANN) to predict the thermal performance of PCM in a 2D cavity	Numerical	Effect of Hartmann numbers, hybrid nanoparticle volume, and porosity of the medium on the melting process	Hartmann number of 40 reduced the charging time by 40%. Maximum 18.5% decrease in the charging time in the presence of hybrid nanoparticles. Reliable prediction of the melting time by ANN modeling approach.
Fan et al. (2021) [63]	Magnetic particles driven by a magnetic field in liquid PCM moving between the solid-liquid interface and the heating surface	Experimental	Effect of particle fraction and magnetic field frequency on the melting process	An experimental correlation for predicting the Nusselt number. Decrease in the melting time by 15.8% in the case of heating surface having 55°C. Maximum enhancement in the heat transfer by 25.4%.
He et al. (2022) [64]	Fe_3O_4-paraffin PCM inside a cavity subjected to uniform magnetic field	Experimental	Effect of nanoparticle concentration and the strength/direction of the magnetic field on the solidification process	Local non-uniformity in the solid phase increased/decreased under positive/negative fields. Positive magnetic field increased the heat flux, energy release, and solid-phase fraction by 29.2%, 19.2%, and 24.8%, respectively. Unmanaged increase in the magnetic induction deteriorating the economic advantage of phase change regulation.
Aly et al. (2022) [65]	Incompressible Smoothed Particle Hydrodynamics (ISPH) method to analyse MHD thermosolutal convection of NEPCMs suspended in a porous wavy cavity containing high-temperature crescents	Numerical	Effect of time-fractional derivative, Hartmann number, nanoparticle concentration, and thermal radiation parameter	Reduction in the movement of NEPCM by increasing the time-fractional derivative, Hartmann number, and solid volume fraction Decrease in the nanofluid speed by 26.3% by increasing the time-fractional derivative, α, from 0.95 to 1. Improvement in the nanofluid movement by increasing the thermal radiation factor.

3.1 Rectangular geometry

Lei et al. [47] dispersed graphene nanomaterials and sodium dodecyl benzene sulfonate (SDBS) in PCM (paraffin), which was then solidified in a rectangular chamber with a vertical orientation. An electromagnetic field was applied with an electric-field intensity of 110 volts and a magnetic induction intensity of 0.1 tesla. The authors found that graphene nanoparticles were dispersed more uniformly throughout the solid region in the presence of electromagnetic field. In another work, Laouer et al. [48] investigated the impact of magnetic field on the melting process of copper-water (ice) as NEPCM inside a rectangular enclosure. The Lattice Boltzmann Method was used in the formulation and resolution of the phase change process. Figure 1 shows the duration of the melting process, which is significantly extended at higher Hartmann number. Adding nanoparticles in the absence of magnetic field increased the liquid fraction, while the opposite trend was observed in case of Hartmann number of 30 and 60. For Hartmann number of 90, the increase in the nanofluid volume fraction improved the liquid fraction. These observations are all valid at Rayleigh number of 10^5. Note that the Rayleigh number is associated with buoyancy-driven flow and effect of natural convection. It is defined as the product of Grashof number and Prandtl number

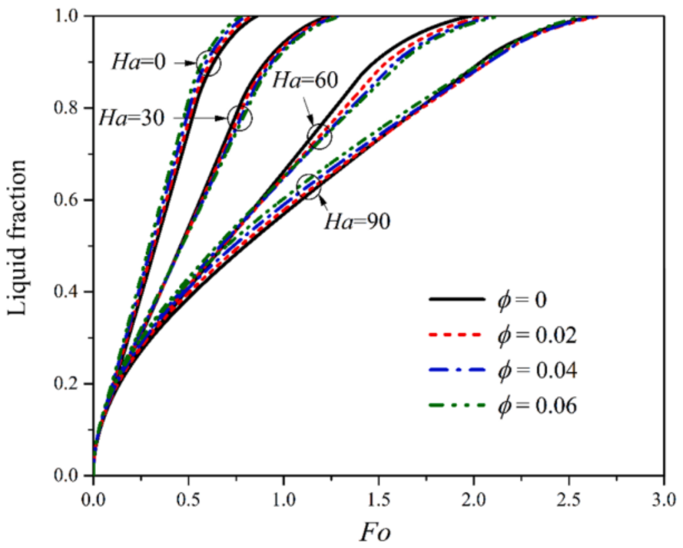

Figure 1. Liquid fraction time evolutions for various Hartmann number (Ha) and nanofluid volume fraction (ϕ) at Rayleigh number of 10^5 (Figure reproduced from [48])

In Figure 1, Fourier number is defined as the ratio of the product of thermal diffusivity and time to the characteristic length scale. The Hartmann number (Ha) is also the ratio of electromagnetic force to the viscous force.

3.2 Cylindrical geometry

Fan et al. [49] intensified the convective heat transfer through employing rotating magnetic field to accelerate the melting performance of 1-dodecanol PCM. As a result, magnetic particles scattered in liquid PCM and moved circumferentially inside the heat reservoir. Under rotational speed of 20 rpm and 1.0 wt% particle fraction as well as heating temperature of 35°C, total melting time shortened by 22.9%. The solid-liquid interface takes the shape of heating surface when the forced convection is more severe. Focusing on non-uniform magnetic field, Farahani et al. [50] evaluated the melting behavior of lauric acid with ferric oxide nanoparticles PCM in a 3D cylindrical container with discrete and continuous innovative fin designs. Introducing non-uniform magnetic field has increased the PCM liquid fraction by 63–72%. The melting rate also intensified by 31.8% and 37.87% for spiral fins and continuous rectangular fins, respectively, as a result of increasing the surface area available for heat transmission. In another work by the same research group, Farahani et al. [51] focused on seven innovative fin configurations to improve the melting performance of PCM in the presence of non-uniform magnetic field. The results demonstrated that the melting fraction can be improved by 1.5–2.5% as a result of increasing the NPVF from 2.5–5%. Further improvement in the melting rate was observed by 16–57% increase in the magnetic field strength.

Saha [52] investigated the solidification and melting procedures of gallium in a semi-circular cavity with a heated circumferential wall subjected to uniform magnetic domain and thermos-capillary effects. A detailed parametric study was conducted over the magnetic field direction, Hartmann number, Rayleigh number, Marangoni number, and gravity conditions. According to this study, the angle of the magnetic field has an insignificant/marginal effect on the solidification/melting of gallium. Under microgravity condition and in the absence of magnetic field, the melting process has been improved by the thermos-capillary convection. The results showed 7.6% reduction in the melting time under 0.05 g and 20.22 °C temperatures difference between the phase change and hot wall. In the presence of magnetic field, the melting time has been extended by 5.48% due to increasing the Hartmann number from 0 to 25 at the magnetic angle of 45°.

Selimefendigil and Öztop [53] investigated the effect of perturbations, bifurcation, and magnetic field on the phase change process of spherical shaped encapsulated paraffin wax PCM inside a cylindrical enclosure. The authors varied the Reynolds number values between 250 to 500, Hartmann number between 0 to 15, the junction place between 0.1H2 to 0.3H2, and nanoparticle concentration between 0.02% to 0.1%. When the Re number increases, the entire phase transition time (t-PC) decreases by about 73% and 26% for bifurcating and flat channels, respectively. At Hartmann number of 15, t-PC decreases by 20% in case of a flat channel, while it increases by 146% in case of a bifurcating channel.

3.3 Square geometry

Kohyani et al. [54] investigated the effect of magnetic field on the melting of nano-PCM inside a porous cavity. Changing the porosity of medium is a more dominant factor in the melting process than varying the nanofluid volume fraction. They reported that a strong magnetic field decreased the charging time and the predominance of conductive heat transfer inside the cavity. Figure 2 shows the melting fraction as a function of Ste.Fo for various Rayleigh numbers. Increasing the Rayleigh number improved the melting rate due to an increase in the convective heat transfer. Figure 3 shows the time history of isotherms and streamlines at constant Rayleigh and Hartmann numbers, nano-PCM volume ratio and medium porosity parameters for three values of Ste.Fo. The power of vortexes and the convection heat transfer increased with time due to increasing the temperature difference between the up and bottom of the cavity.

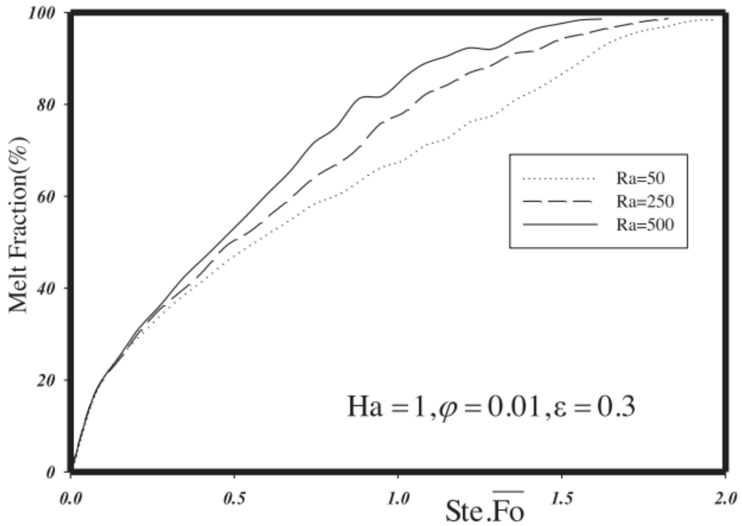

Figure 2. Melt fraction as a function of Ste.Fo for various Rayleigh numbers (Figure reproduced from [54])

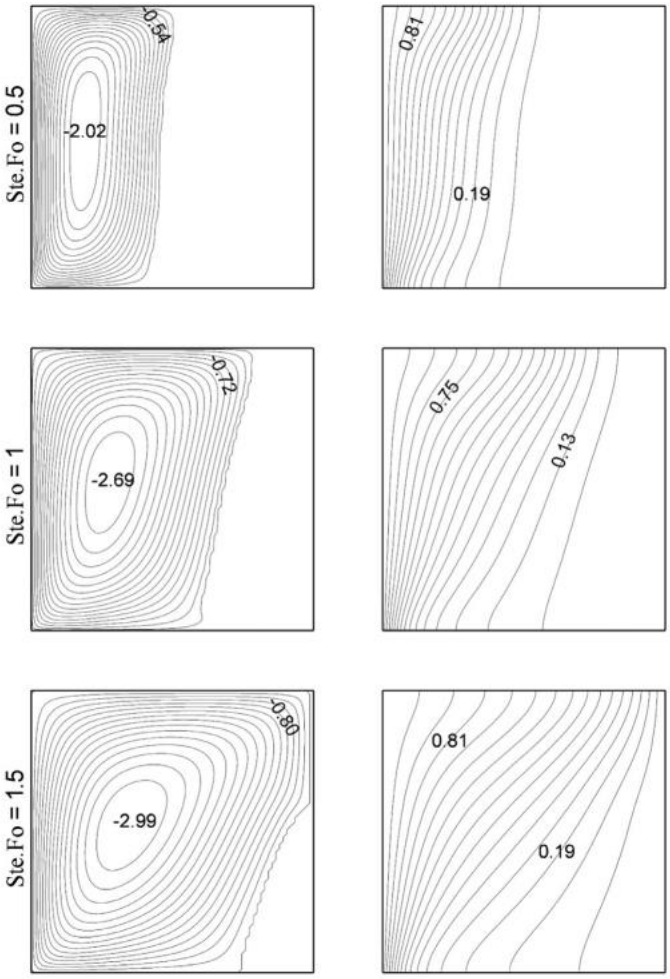

Figure 3. Streamlines (left) and isotherms (right) at fixed Rayleigh number of 100, Hartmann number of 1, nano-PCM volume ratio of 0.01, and medium porosity of 0.3 (Figure reproduced from [54])

Ghalambaz et al. [55] investigated the non-Newtonian behavior of a Ferro- and magneto-hydrodynamic PCM during the melting process. They performed a detailed parametric study over the Rayleigh number ($10^4 < Ra < 10^6$), the Hartman number ($0 < Ha < 250$), the Power-law index ($0.7 < n < 1$), and the magnetic parameter ($0 < Mn_f < 7000$) on the normalized melt volume fraction (NMVF), melting front, and the Nusselt number. Figure 4 shows the variation of NMVF with Hartman and magnetic parameters. An increase in the Hartman and magnetic parameter decreased and increased the NMVF at different levels depending on the power-law index. In the presence of magnetic field, the increase in power-law index worstened the NMVF since the flow field is influenced by Lorentz force. Increasing the magnetic field parameter decreases the melting time due to an increase in the convection heat transfer of the flow field.

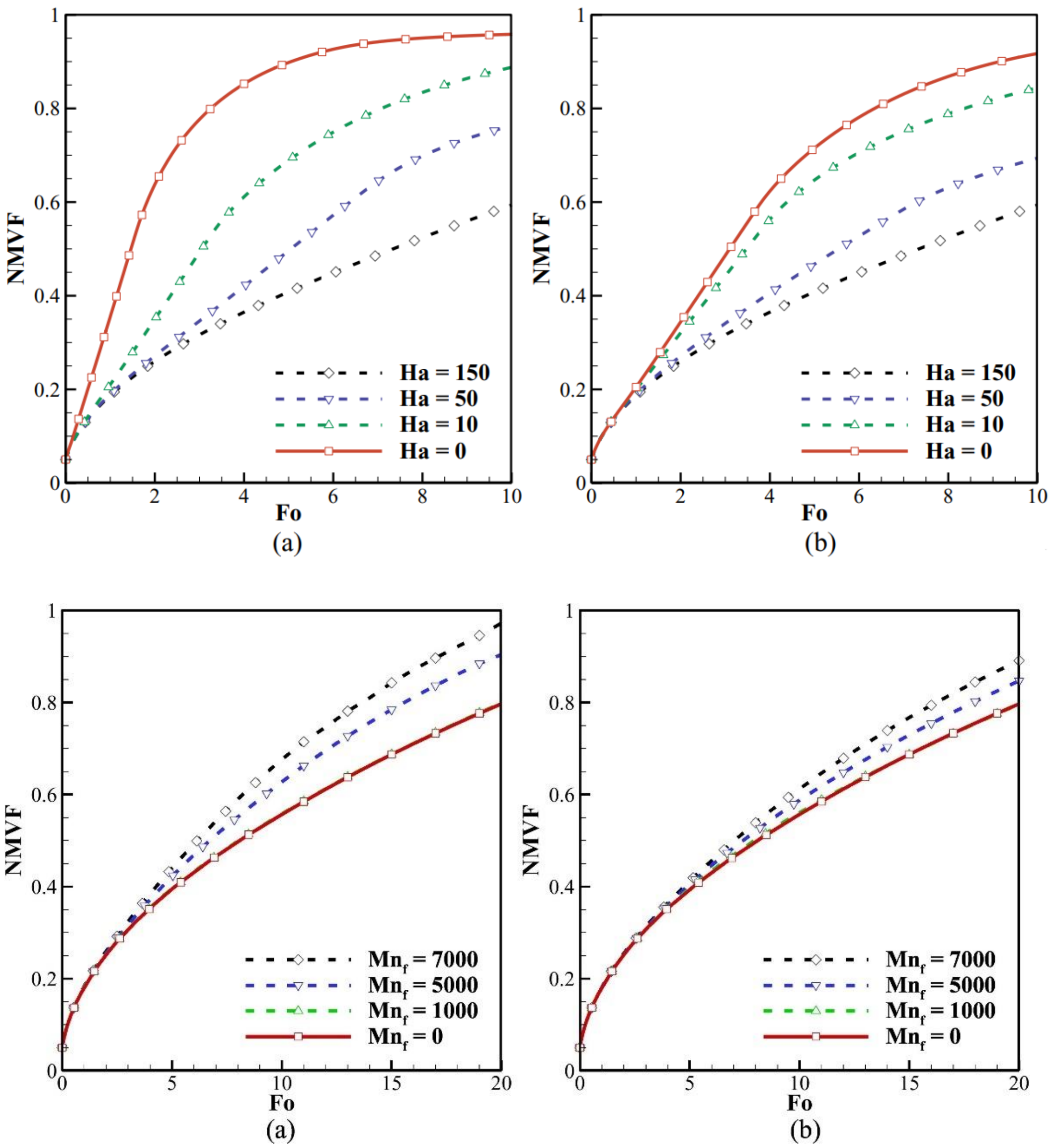

Figure 4. Variation of NMVF with Hartman and magnetic parameters for power index of (a) 0.7 and (b) 1 (Figure reproduced from [55])

Mehryan et al. [56] examined the impact of two magnetic sources with different strengths on the melting process of PCM inside a cavity. The authors used Galerkin FEM together with Lagrangian-Eulerian to solve the governing equations. The intensity ratio of these magnetic fields (γ_r) has significantly affected the melting front. Between the two parameters being magnetic and Hartman number, the latter has a more impact on the progress of the melting front. Figure 5 shows the melting fraction of PCM with Fourier number for different magnetic fields. As seen in this figure, the melting rate is consistent up to Fourier number of 1.5. Beyond this point there was a reduction in the melting fraction by increasing the magnetic field due to the increase in the flow vortices.

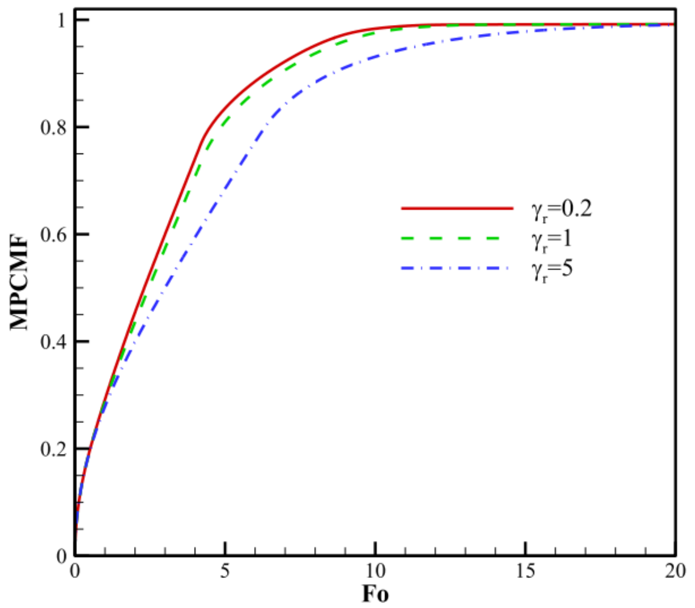

Figure 5. Variation of the charging PCM fraction with Fourier number for different γ_r (Figure reproduced from [56])

Kumar et al. [57] studied the melting of paraffin PCM) with copper (Cu) nanoparticles in square cavity subjected to a constant external magnetic field in the horizontal direction. The free convection is suppressed when magnetic flux is employed in electrically conducting PCM. The energy storage capacity decreased by ~9% by increasing the Hartmann number from 0 to 40. The maximum melting rate and energy storage capacity of NEPCM were found at 2% and 0.5% nanoparticle concentration, respectively.

3.4 Annulus geometry

The influences of non-uniform magnetic fields on the charging and discharging of NEPCM in an annular domain were mathematically studied by Dibavar et al. [58]. A wire that carries an electrical current inside the annulus central point was used to create the magnetic field. Based on the results, the melting and solidification time reduced by 39.9% and 14.3% in the presence of magnetic field. Figure 6 shows the effect of magnetic field on the melting and solidification performance of ferrofluid in a non-electrical conductive field. From this figure, it is evident that the increase in the magnetic field had a more dominant effect on the charging than the discharging process at a constant Hartmann number and Rayleigh number. that an increase in the Hartmann number causes a significant reduction of the melting and solidification speeds.

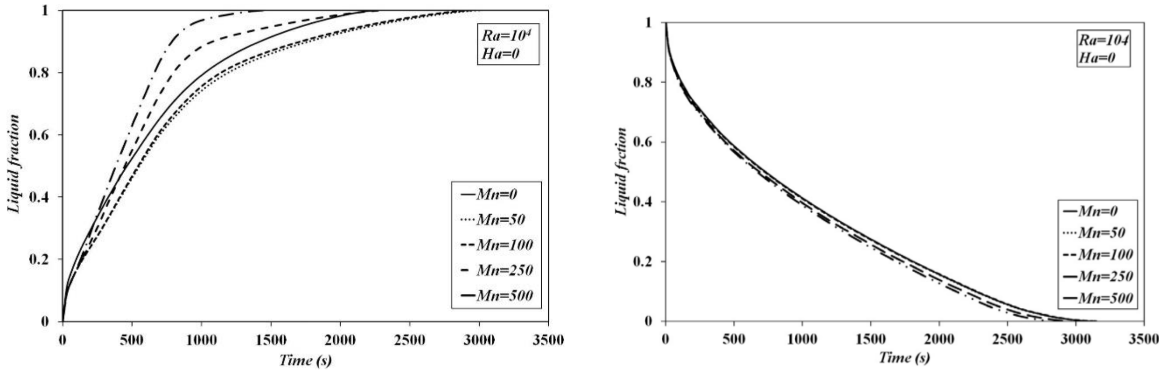

Figure 6. Liquid fraction time evolution in the charging and discharging process of 5% volume fraction ferrofluid in a non-electrical conductive field at various strengths of a magnetic field (Figure reproduced from [58])

Sheikholeslami and Mahian [8] simulated the impact of magnetic field on the solidification rate of CuO nanoparticles PCM inside a porous energy storage device. They analysed the role of Lorentz forces, Rayleigh number, and nanofluid concentration on the solidification process of NEPCM. Figure 7 shows the solid fraction at different Rayleigh and Hartmann numbers at 4% nanofluid concentration. The solidification time reduced by 23.5% when the Hartmann number increases from 0 to 10. Increasing the Rayleigh number from 0 to 100 reduced the solidification time by almost the same percentage. The addition of nanoparticle by 4% volume fraction into the PCM reduced the solidification time by 14%.

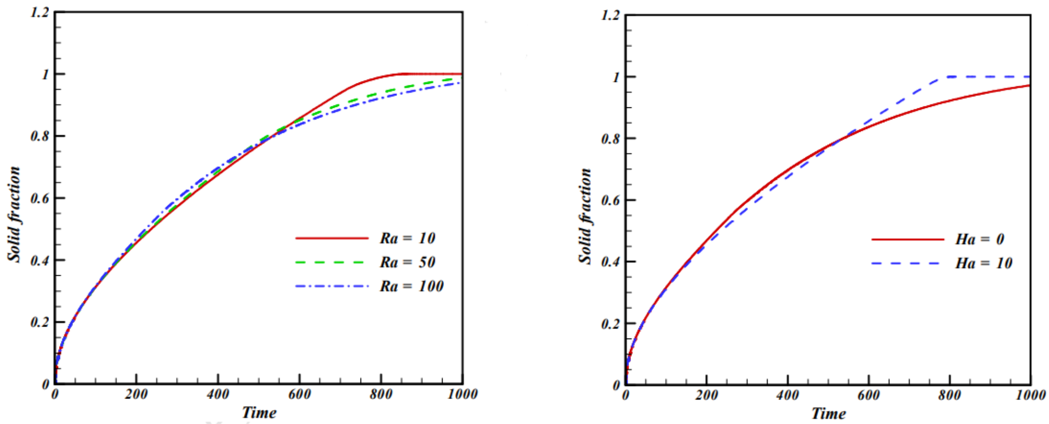

(a) Ha=0 (b) Ra=100

Figure 7. Variation of solid fraction with time at 4% nanofluid concentration for various (a) Rayleigh and (b) Hartmann numbers (Figure reproduced from [8])

3.5 Other geometries

In the presence of a magnetic field, Sheikholeslami [59] used the finite element method (FEM) to model the discharging of NEPCM. The Darcy and Koo–Kleinstreuer–Li (KKL) models were used to analyse nanofluid and porous media. The findings demonstrated that the growth in the Hartmann number would decrease the solidification time.

Ghalambaz et al. [60] studied the heat transfer and melting of electrically conductive phase transition materials subjected to a magnetic field inside of a hollow domain. The sides of the hollow were isothermal, while the higher and lower walls of the enclosure were adiabatic. The hot wall temperature was greater than the fusion temperature of PCM, whereas the cold wall temperature was less than or equal to fusion temperature. The role of magnetic field is more pronounced by progressing with melting time. Changing the location of magnetic force from bottom to middle of the cavity has a significant influence on reducing the non-dimensional melting time by 13.5%.

Through a 3D transient numerical simulation, Shi et al. [61] evaluated the melting and solidification performance of paraffin type A16 with Fe_3O_4 nanoparticles inside a shell and multi-tube latent heat thermal energy storage. The complete melting and solidification time has been decreased by 80.0% and 53.2%, respectively, through applying magnetic field with 50 mT intensity. The solidification time took longer than the melting time due to the formation of a solidified layer on the outer surface of the tube, acting as an insulation layer between HTF and PCM. The authors reported that the presence of magnetic field can decrease the difference between the melting and solidification time, which is essential for a cyclic melting/solidification processes.

Selimefendigil and Öztop [62] applied a uniform magnetic field in radial direction and field with different magnitudes in various regions of the computational model to assess the melting performance of PCM-filled vertical cylinder. Imposing the magnetic field has accelerated the charging process and phase transition near the walls. Charging time can also be shortened by 40% and 14.5% with increasing the Hartmann number to 40 of the magnetic field in the PCM domain and other domains, respectively. The authors developed a predictive modeling approach to predict the melting time as a function of the magnetic field and volume fraction of hybrid particles.

Applying a uniform magnetic field has a significant role in controlling the convective heat transfer. Fan et al. [63] was the first who analysed the melting process of PCM under alternating magnetic force. Intensified forced convection was induced in the liquid PCM as a result of magnetic particles travelling between the solid-liquid interface and heating surface under alternating magnetic force (see Figure 4). The suggested method reduced the PCM melting time by 15.8% when the heating surface temperature was set at 55 °C. The maximum increment of the overall heat transfer coefficient between the heating surface and the solid-liquid interface was 25.4%.

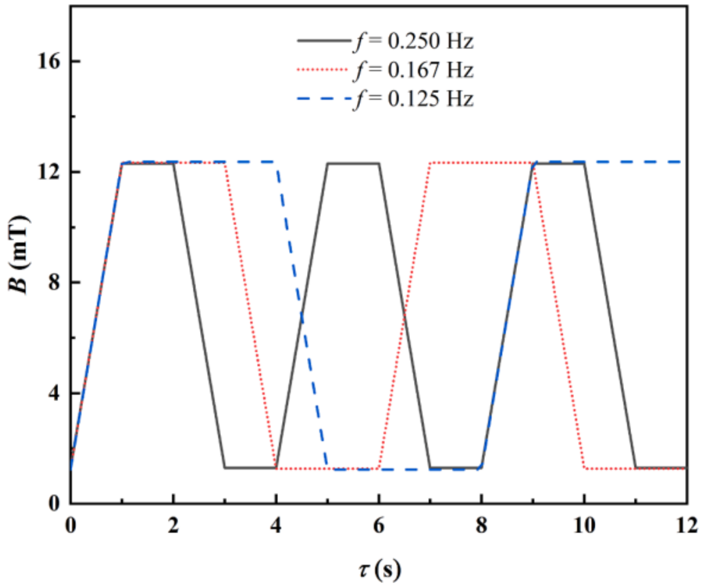

Figure 8. Induction intensity of magnetic field in the center of heating surface (Figure reproduced from [63])

The enthalpy porosity method was intensively used by several scholars to model solid-liquid phase change process. However, He et al. [64] switched to thermo-magnetic convection model to analyse the solidification behavior of paraffin wax PCM with Fe_3O_4 nanoparticles under a uniform magnetic field. Depending on the magnetic field direction, the solidification process was either enhanced or deteriorated. The amount of energy released and the solid fraction were decreased and increased by 4.6% and 3.9%, and by 29.2% and 19.2%, under positive or negative fields, respectively, due to the different nanoparticles motion pattern dominated by Kevin force.

Aly et al. [65] studied the effects of thermal energy on Magnetohydrodynamic (MHD) thermosolutal convection of NEPCMs suspended in a horizontal wavy porous cavity with embedded high-temperature crescents. Incompressible Soft Particle Hydrodynamics (ISPH) was employed to solve the governing equations. The increase in time-fractional derived, Hartmann number, and solid size reduced the NEPCM motions. An increase in time-fractional derivative from 0.95 to 1 slowed down the speed of nanofluid by 26.3%.

4. Effect of rotation

Storage rotation is identified as an active heat enhancement approach to accelerate the charging and discharging performance of PCMs/NPCMs. This can be achieved through the use of flexible pipes and couplings, which enables the rotation of storage medium in less than one circle. Table 2 lists the geometrical, operating conditions, and key take-away findings of recent studies addressing the role rotation on the melting/solidification procedures of PCMs/NEPCMs inside an enclosure with different geometries. The citation list [66–73] focuses on this importance in different geometries as summarized in the following subsections.

Table 2. A summary of studies on the effect of rotation on the melting/solidification procedures of PCMs/NEPCMs inside an enclosure with different geometries

Authors (year)	**Configuration**	**Type of study**	**Studied parameters**	**Highlighted results/findings**
Khosroshahi and Hossainpour (2021) [66]	PCM filled in the annulus of a 2D double-pipe LHTES	Numerical	Effect of TES rotational speed and rotation scenario on the melting process	Reduced melting time by 3.45% under constant rotational speed compared to fixed operation. Maximum 15.5% reduction in the melting time through applying two opposite rotations considering 180° difference between the stop ends.
Kosroshahi and Hossainpour (2022) [67]	2D double-pipe with paraffin PCM in the annulus	Numerical	Effect of straight fins and TES rotation in 7 combinations on the melting process	Reduced melting time by 18.5% and 70% through employing TES rotation and fins. Optimal 72% decrease in the melting time by simultaneous use of both techniques.
Fathi and Mussa (2021) [68]	Paraffin wax PCM in a horizontal shell-and-tube LHTES	Experimental	Effect of rotational speed on the melting process	Marginal enhancement in the melting process under 9 rpm rotational speed, experimental limit of the rotation. Understanding the trade-off between moving to higher rotational speed and energy implications as the future work.
Soltani et al. (2021) [69]	N-eicosane PCM in a 2D cylinder enclosure containing fins	Numerical	Effect of adding fins in the inner cylinder and rotational speed of the HTF tube on the melting and solidification processes	Reduction in the solidification time by 83.21% through employing tube rotation mechanism. 12.89 W heat transfer rate at 1 rpm rotational speed. Improvement in the heat transfer ratio by 3.87 and 2.45 times in the solidification and melting processes, respectively.
Modi et al. (2022) [70]	Paraffin PCM in a 3D shell-and-tube LHTES	Numerical	Effect of intermittent rotation on the melting and solidification processes	Improved melting by 64–74% through employing bottom eccentricity of 0.6–0.75. Optimal top eccentricity between -0.15 and -0.3 for the discharging process 0.3 as the optimal eccentricity for both the charging and discharging processes.
Yang et al. (2022) [71]	PCM filled into a shell-and-tube LHTES considering heat conduction over the external shell	Experimental	Effect of different rotation mode including rotate, static, and flip on the melting process	Increase and then decrease in the melting time through the flipping time—with the optimal flipping time of 0.375. Shorten melting time by 35.42% accompanied by increase in the TES rate by 54.5%. Better melting performance under rotation mode, 19.35% reduction compared to the optimum flipping condition.
Farsani et al. (2020) [72]	Paraffin wax PCM in a rectangular cavity container	Numerical	Effect of Taylor number and Rayleigh number on the melting process	Rotating cavity in a counter direction of buoyancy flow improved the melting rate by 8%.
Alhashash and Saleh (2022) [73]	Free convection in a square enclosure filled with NEPCM subjected to counterclockwise rotation in the longitudinal direction	Numerical	Effect of rotational speed and NEPCM volume fraction on the melting process	Enhancement in the heat transfer rate by declining the Taylor number and rising the Stefan number. Less phase change and delayed heat transfer under higher rotational speed.

4.1 Annulus geometry

Khosroshahi and Hossainpour [66] developed a double-pipe LHTES unit with a PCM-filled annulus and a storage rotation mechanism to accelerate the charging of PCMs. Constant-speed and stepwise rotations were examined. The results revealed that storage rotating with a constant rotation rate had a low impact on the required time of melting. However, using a step-by-step rotation scenario reduced the charging time by 15.5% compared to the fixed mode. In another study by the same research group, the authors established a two-dimensional model to investigate the feasibility of a new simultaneous utilisation of storage rotation and longitudinal fins techniques to decrease the melting rate and increase the amount of energy stored in a double-channel heat exchanger [67]. Following a detailed analysis of several scenarios, the authors found that embedding the fin on the bottom half of the fixed storage was a more effective pathway to speed up the melting process. The melting time reduced by 72% through employing both heat transfer enhancement techniques.

4.2 Shell-and-tube and cylindrical geometries

Fathi and Mussa [68] conducted a specific study to determine how the rotation of the tube can affect the productivity of the LHTES. While water served as the HTF, paraffin (C_nH_{2n+2}) was employed as the PCM in this experiment. The trials were carried out at three different rotational speeds (i.e., 3, 6, and 9 revolutions per minute (rpm)). The findings were compared against those obtained from the stationary case. Rotating the tube at the above-mentioned range of speeds increased the percentage of the liquid fraction by 8.12% after about 11 hours of simulation. Using enthalpy porosity method, Soltani et al. [69] simulated the effects of fins and rotation on the solidification and melting of PCM. Figure 9 shows the effect of rotational speed on the liquid fraction of PCM. It is observed that solidification time greatly reduced, by 83.2%, at higher rotational speed. From this analysis, the authors reported that there was direct relationship between the rotational speed and heat transmission from and to PCM—leading to a maximum heat transfer ratio enhancement by 3.9 and 2.5 times during discharging and charging processes.

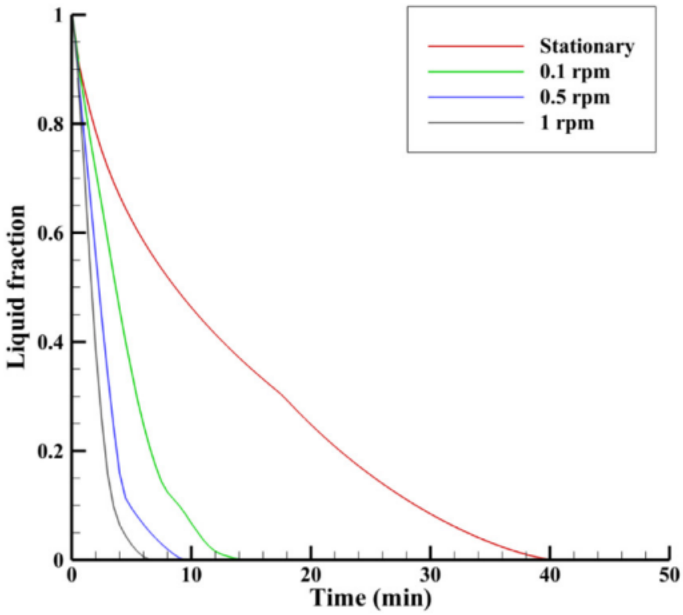

Figure 9. Liquid fraction time evolution in the discharging process of PCM at various rotational speeds (Figure reproduced from [69])

Modi et al. [70] studied the effect of eccentric inner HTF tube placements on a shell-and-tube LHTES system during solidification and melting. Intermittent LHTES unit rotation was suggested to effectively boost both the solidification and melting processes. Bottom eccentricity helped the melting process but hindered solidification. The unique rotating approach efficiently fitted bottom eccentricity to increase melting while top eccentricity to improve solidification. In the continuation of this work, a visual experimental examination was carried out by Yang et al. [71] to naturally assess the establishment impact of several rotation methods (static, rotate, and flip) and enhance the flipping duration with low extra energy consumption. The temperature distribution and phase interface location were explored under a variety of rotating settings and at a range of various input temperatures while considering the conductivity of the outer shell. The findings indicated that the charging time of LHTESU first increased and then decreased with the rise of the flipping period. When the dimensionless flipping time was equal to 0.375, the melting performance was at its highest possible level.

4.3 Rectangular and Square geometries

Farsani et al. [72] numerically examined PCM charging in a tracking solar panel cavity. The cavity was filled with paraffin and rotated steadily. Melting and heat transmission were influenced by buoyancy-driven flow and rotational parameters. When rotation occurred contrary to buoyancy-driven flow in molten fluid, heat transmission and melting rate increased by up to 8%. Figure 10 shows the liquid fraction time evolution in the charging process for cases with/without Coriolis force and rotational buoyancies at two Rayleigh numbers. The results showed that the melting rate increased by about 2% through employing rotational buoyancies and Coriolis force.

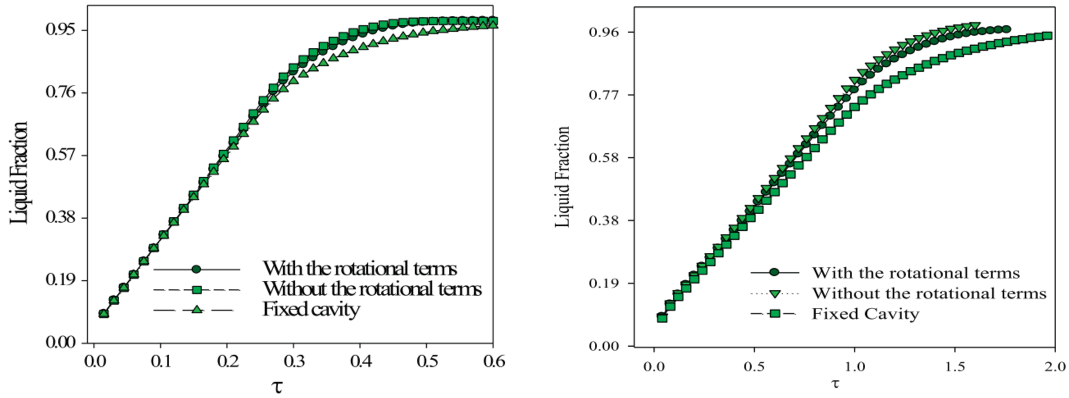

Figure 10. Liquid fraction time evolution in the charging process for the cases with/without Coriolis force and rotational buoyancies for Rayleigh number of 2.72×10^6 (left) and 5.74×10^5 (right) (Figure reproduced from [72])

Alhashash and Saleh [73] investigated the possibility of a thermal natural convective in hybrid nanofluids contained in a square container. The angular velocity of the enclosure was maintained at a constant counterclockwise direction. The results indicated that by raising the rotational speed, the amount of NEPCM undergoing phase change reduces—which slowed down the heat transmission. The authors also found that higher Stefan number and lower Taylor number leads to higher heat transfer rates.

5. Effect of tilt angle

During the procedure of melting PCM in a variety of configurations, there have been many practical and numerical investigations that have shown that buoyancy-driven convective heat transfer and orientation of the enclosure play an important role on the melting and solidification processes. A few studies have looked at the possibility that tilting the enclosure might change the form of the convection currents and, as a result, the PCM charging process [71]. Table 3 lists the geometrical, operating conditions, and key take-away findings of recent studies addressing the role tilt angle on the melting/solidification procedures of PCMs/NEPCMs inside an enclosure with different geometries. The citation list [74 – 90] focuses on this importance in different geometries as summarized in the following subsections.

Table 3. A summary of studies on the effect of tilt angle on the melting/solidification procedures of PCMs/NEPCMs of an enclosure with different geometries

Authors (year)	**Configuration**	**Type of study**	**Studied parameters**	**Highlighted results/findings**
Sharifi et al. (2013) [74]	PCM positioned concentrically inside a 3D vertical cylindrical container with outward melting	Experimental and numerical	Effect of tilting angle on the melting process	Strong effect of 3D geometry at the tilting angle of 5°. Substantial impact of inclination angle on the local temperature of the PCD.
Allen et al. (2014) [75]	PCM/NEPCM contained in a cylindrical enclosure with heat transfer occurring through a solid copper rod or a heat pipe (HP)—the latter is combined with foam and aluminum foils	Experimental	Effect of inclination angle and different configurations—including HP-Foam-PCM, HP-Foil-PCM, HP-PCM, Foam-PCM, Rod-PCM, and NEPCM— on the melting and solidification processes	Higher liquid fraction for Rod-PCM and HP-PCM in a horizontal orientation. Marginal improvement in the liquid fraction for HP-Foam-PCM and HP-Foil-PCM in a vertical orientation. Reduced melting and solidification time by 11% an 3% in case of HP-Foil-PCM compared to NEPCM irrespective to orientation.
Siyabi et al. (2019) [76]	Paraffin PCM inside a 2D cylindrical heat exchanger storage system	Experimental and numerical	Effect of tilting angle on the melting process	Reduction in the temperature difference as a result of an increase in the inclination angle. Faster melting in the inclination angle of 45°, 13% lower than 0° angle. Shorter PCM melting time when the movement of liquid PCM is in the same direction to that of buoyant force.
Zennouhi et al. (2016) [77]	Galium PCM inside in a 2D rectangular cavity	Numerical	Effect of tilting angle on the heat transfer and fluid flow structure during the melting process	Enhancement in the melting rate by reducing the title angle from 90° to 0°. Formation of Bénard convection cells in the liquid region of the solid-liquid interfaces.
Joneidi et al. (2017) [78]	RT35 PCM inside two designated holes at the right and top side of a rectangular enclosure	Experimental	Effect of tilting angle and heat flux of the heater on the melting process	Reduction in the melting time by increasing the heat flux. Increase in the angle of the heater was accompanied by increase in the melting time and the amount of energy stored in TES.
Kamkari and Groulx (2018) [79]	Lauric acid PCM in a finned rectangular side-heated enclosure	Experimental	Effect of tilting angle and number of fins on the melting process	Higher melting rate at lower inclination angle for both finned and un-finned cases. Minimum melting time in case of a horizontal enclosure with 3 fins. Orientation as a more influential factor than adding fins in terms of enhancing the heat transfer rate and shortening the charging time.
Abdulmunem et al. (2020) [80]	Paraffin PCM contained in a rectangular container	Experimental and numerical	Effect of tilting angle on the melting time	Prolonged melting process at lower inclination angle. Minimum melting time of 108 minutes at 90° tilt angle.
Abdulmunem et al. (2021) [81]	PCM as heat sink in the backside of a rectangular PV cell	Experimental and numerical	Effect of tilting angle on the melting process and PV cell temperature	Acceleration in the melting process by increase in an inclination angle. 12% decrease in the PV cell temperature at an inclination angle of 90°.
Kousha et al. (2016) [82]	Paraffin PCM in a shell-and-tube heat exchanger	Experimental	Effect of Stefan number, Reynolds number, inclination angle, and	More melting rate within the first half of the domain in the horizontal than the inclined orientations.

			Grashof number on the melting and solidification processes	Higher heat transfer rate in the vertical orientation during the discharging process. Insignificant influence of angle change on the solidification performance.
Shen et al. (2019) [83]	RT60 PCM in a vertical shell-and-tube heat exchanger	Numerical	Effect of tilting the lateral surface angle and Reynolds number on the melting and solidification processes	Improved/worsened the melting/solidification by increase in the tilting lateral surface angle. Reduction in the melting time by 45% at 7° compared to 0° tilting angle 4° as the optimal angle to reduce the melting and solidification time by 22% and 8.5%.
Avci and Yazici (2018) [84]	N-eicosane PCM in a flat heat sink exposed to a constant heat flux	Experimental	Effect of tilting angle on the thermal performance of the melting process	Significant effect of tilting effect on the thermal performance of a heat sink with PCM compared to a case without PCM. 5.5 times higher operating time for a heat sink with 90° tilting angle compared to 0° angle.
Karami and Kamkari (2018) [85]	Dodecanoic acid PCM placed inside a finned enclosure	Numerical	Effect of tilting angle and number of fins on the melting and solidification processes	Shortened melting time at lower inclination angle due to improvement in the natural convection. Maximum melting time reduction of 72% in case of 0° angle with 3 fins. Intensified heat content by decrease in the number of fins and increase in the tilting angle.
Ghalambaz et al. (2020) [86]	Non-Newtonian n-octadecane PCM with a mesoporous silica particles inside a 2D inclined container	Numerical	Effect of nanoparticle mass fraction and inclination angle on the melting process	Decrease in the latent heat capacity due to the presence of nanoparticles. Up to 50% reduction in the heat transfer at 5% nanoparticle mass fraction 80% reduction in the heat transfer at -75° tilting angle.
Sorour et al. (2021) [87]	PCM placed in the annulus of a double-pipe heat exchanger	Experimental and numerical	Effect of tilting angle on the melting process of the PCM with various thicknesses	Optimum inclination angle of 45° for the PCM with 14.5 mm thickness, leading to 18% reduction in the melting time. Horizontal orientation resulting in the least charging time for PCMs with small thickness.
Kothari et al. (2021) [88]	Paraffin PCM in a heat sink with/without plate fins	Experimental	Effect of tilting angle and heat flux on the melting process	Prolonged operating time at lower inclination angle both finned and un-finned cases. 44% and 30% decrease in the melting time through reducing the angle from 90° to 0° for un-finned and finned cases.
Yang et al. (2021) [89]	PCM embedded in metal foam inside a cavity with different aspect ratio	Experimental and numerical	Effect of tilting angle and cavity aspect ratio on the melting process	Negligible impact of inclination angle on the melting time/rate at a given aspect ratio. Higher temperature uniformity at a smaller aspect ratio, ~5 times greater in aspect ratio of 0.1 compared to 8.
Wang et al. (2022) [90]	Lauric acid as the PCM in a micro-heat pipe array LHTES unit	Experimental	Effect of tilting angle on the coupled heat transfer between PCM and heat pipe and eventually on the melting process	Decrease in the tilting angle from 90° to 15° was associated with 15.5% heat transfer enhancement and 1.9% increase in the melting time. First decrease and then increase in the heat pipe effective thermal conductivity under a tilting angle ranging from 30° to 90°. Deterioration in the heat transfer under heat flux greater than 30 W and tilting angle lower than 30°.

5.1 Cylindrical geometry

In an experimental study by Sharifi et al. [74], the authors focused on the effect of tilting angle on outward charging of a PCM as a result of a heated rod positioned inside a cylindrical enclosure. They also developed a two-dimensional model of the geometry for predicting the melting process for the non-tilted case. The results showed that a little tilting of the test cell had an extensive impact on the local temperature distribution inside the PCM. This was due to the three-dimensional nature of the experiments, which required a three-dimensional model to better capture the PCM melting. Allen et al. [75] experimentally tested the influence of tilt angle on PCM melting and solidification. Heat transfer occurred through a concentrically located heat pipe (HP) or solid copper rod and an underlying copper disc. Six configurations were investigated: HP-Foil-PCM, HP-Foam-PCM, HP-PCM, Rod-PCM, Foam-PCM and non-enhanced PCM. Due to conduction being the major mechanism of heat transport, experimental data showed that unit direction had a small influence on discharging rates in all cases. For the charging, the orientation of the enclosure had a higher effect due to higher impact of natural convection. Figure 11 shows the effect of ΔT and enclosure orientation on the liquid fraction during the melting process. It should also be noted that the orientation of the container has a significant impact on the charging process. Moreover, the effect of orientation is lower at higher ΔT. The authors concluded that the charging process is more influenced by the tilting angle than the discharging process.

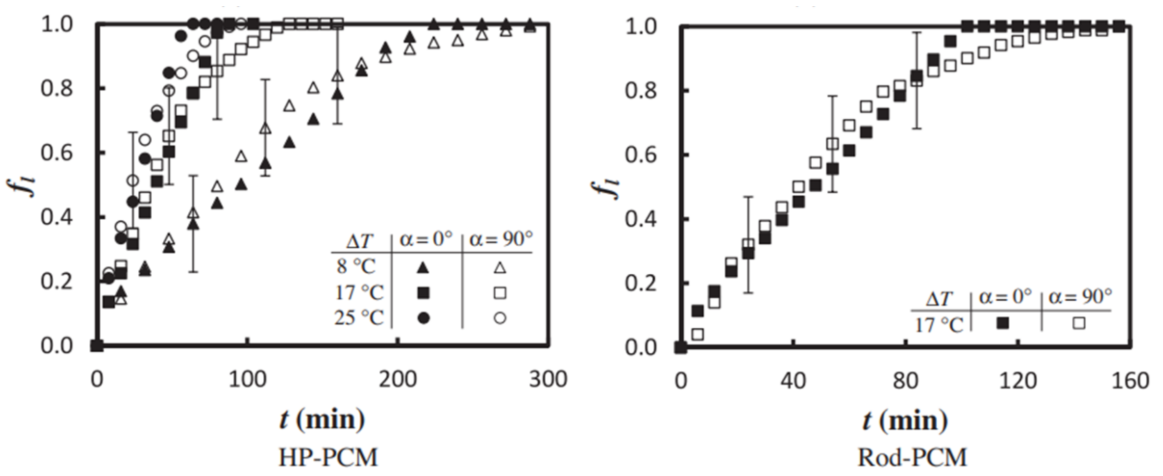

Figure 11. Effect of ΔT and container orientation on the liquid distribution during the charging process for HP-PCM and Rod-PCM cases (Figure reproduced from [75])

Siyabi et al. [76] used experimental and computational methods to study the Paraffin wax PCM melting under various tilting angles. PCM melting behavior within the storage was defined by the distribution of temperature, melting profiles imaging, thermal stored rate, and liquid stream of PCM. The PCM storage inclination angle affects temperature profile, charging period, and profile. The melting process is faster in the axial than radial direction in the 0°, while opposite trend was observed in 90°. Figure 12 shows that PCM stored at 45° from the horizontal had a higher melting rate compared to that of 0° and 90° because the melting behavior exhibited a similar rate in both directions. The results of numerical simulations indicate that the direction of buoyant force resulting from the melted liquid PCM had a major role in both melting rate and melting direction within the PCM storage.

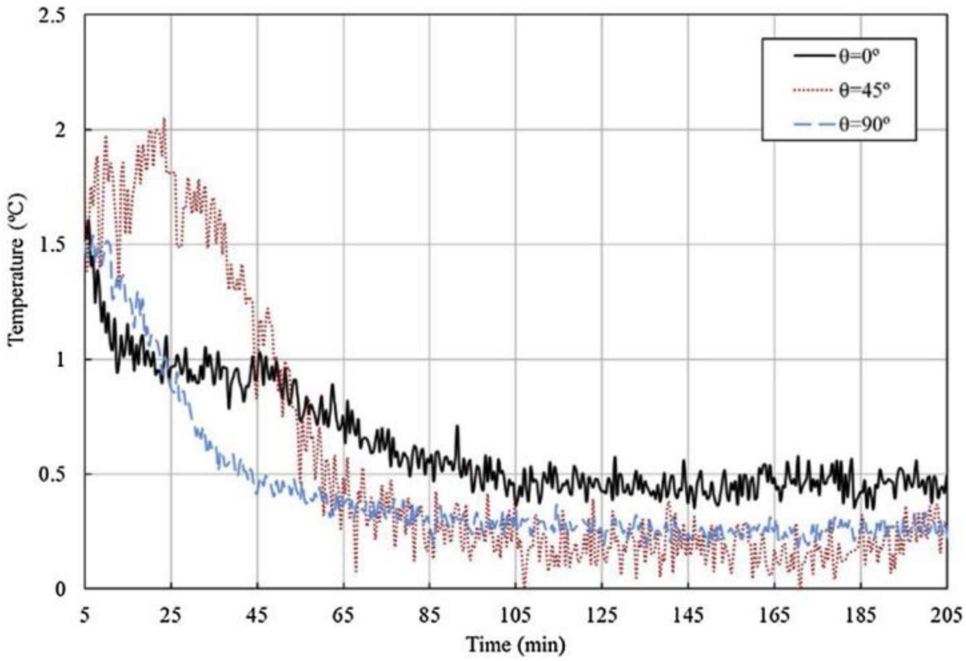

Figure 12. Variation of HTF temperature with time for various tilting angles of PCM storage (Figure reproduced from [76])

5.2 Rectangular geometry

Zennouhi et al. [77] conducted a numerical simulation to assess the melting behavior of Galium PCM in a rectangular cavity under different tilting angles. Natural convection related to phase change was solved utilising a shapeless mesh, finite-volume approach, and enthalpy porosity methodology. Figure 13 shows the liquid fraction time evolution of PCM with respect to various tilting angles. As seen in this figure, the charging rate and, as a result, the liquid fraction increases by reducing the inclination angle. This is mainly due to the natural convection regime, which prevents the development of melting process at higher inclination angles. Bénard convection cells are generated in the liquid phase by carefully evaluating the solid-liquid interfaces.

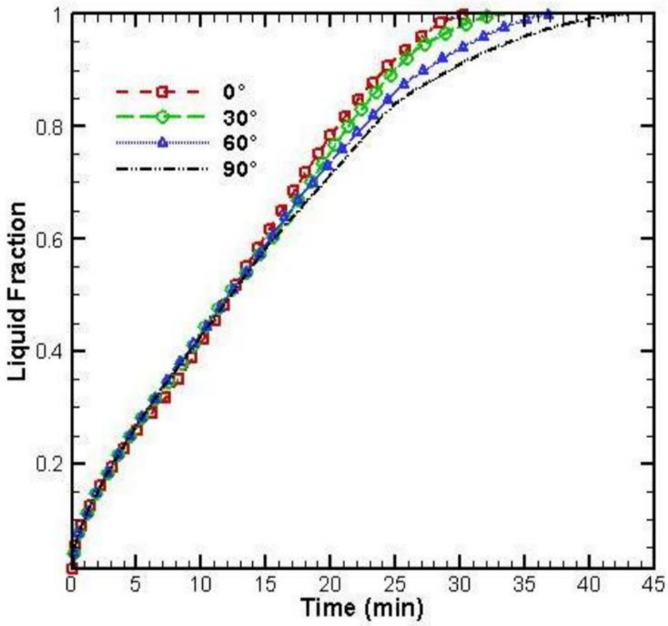

Figure 13. Liquid fraction time evolution in the charging process of PCM for various tilting angles (Figure reproduced from [77])

Joneidi et al. [78] studied the effect of heating power and inclination angle (i.e. 0, 45, 90°) on the melting time of RT35 PCM in a rectangular cavity. The domain was heated through the lower plate. Canon G9 camera used to capture the changes in the liquid-solid interface. Figure 14 shows the mean average temperature of PCM, melt fraction, and average temperature of heater surface under various heating power and tilting angles. It is evident that increasing the heating power reduces the melting time and increases the mean average temperature of heating surface and PCM. Switching to higher inclination angles resulted in the accumulation of energy at the top of the rectangular cavity, which in turn increased the melting time and mean temperature of both heating surface and PCM. They concluded that the minimum melting time was achieved in an enclosure with a horizontal orientation.

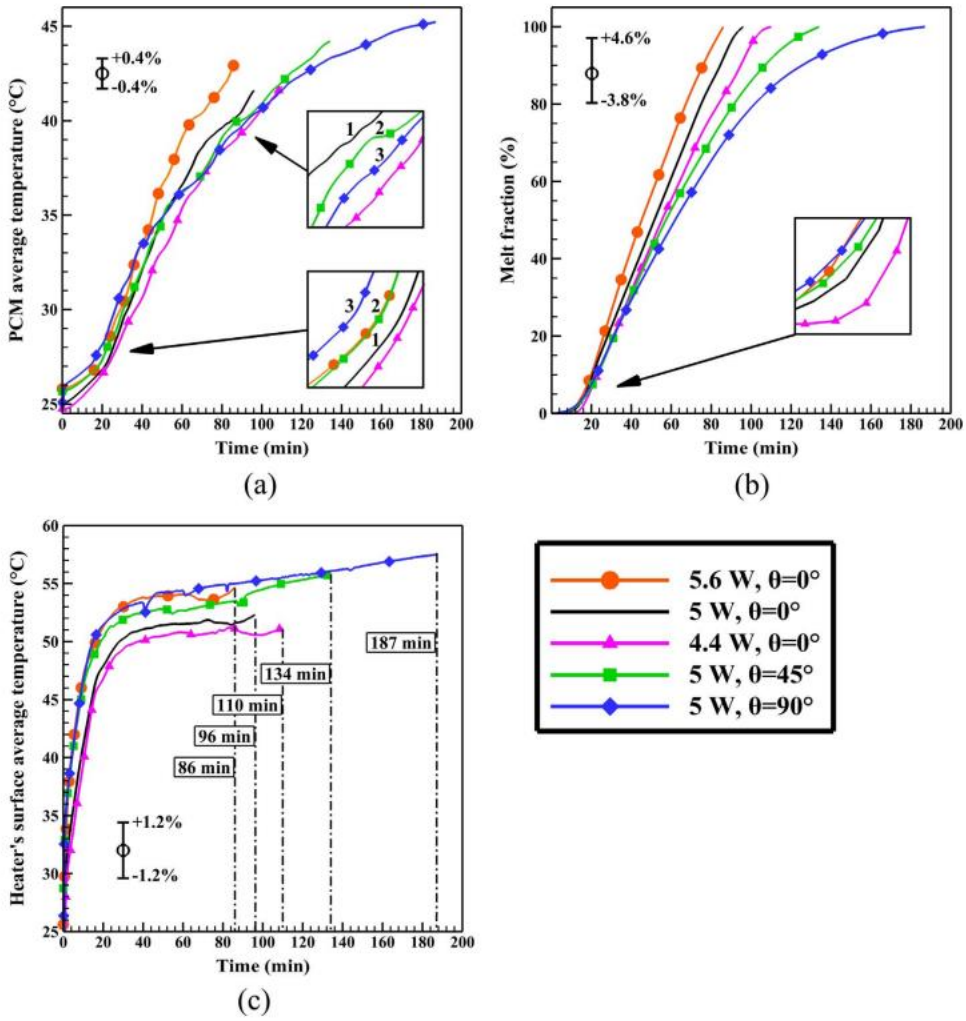

Figure 14. Mean average temperature of PCM, melt fraction, and average temperature of heater surface under various heating power and tilting angles (Figure reproduced from [78])

Kamkari and Groulx [79] studied the effect of adding fins together with inclination angles on the melting behavior of PCM in a rectangular enclosure. In this study, lauric acid melting in side-heated containers with variable numbers of fins was tested at 90°, 45°, and 0° inclination angles. The solid-liquid interface evolution showed higher melting rates at lower inclination angles for both finned and un-finned cases. Figure 15 shows the melting enhancement ratios as a function of time for different inclination angles and number of fins. In all the cases, there is a sharp increment in this ratio within the first few minutes of the melting process—stronger in the case of inclined enclosures with fin—attributed to vortical flow structures in the conduction-to-convection transition. This is followed by a reduction in this ratio after ~40 minutes—more pronounced in the finned cases—as a result of higher thickness of the PCM liquid layer that impeded the convection flow inside PCM. The results corroborated the findings of other researchers regarding better melting rate at reduced inclination angle even in case of finned configurations. Among the cases analysed, the maximum melting enhancement ratios of 3.7 was achieved in the 3-fin configuration—equivalent to 115% improvement in the heat transmission.

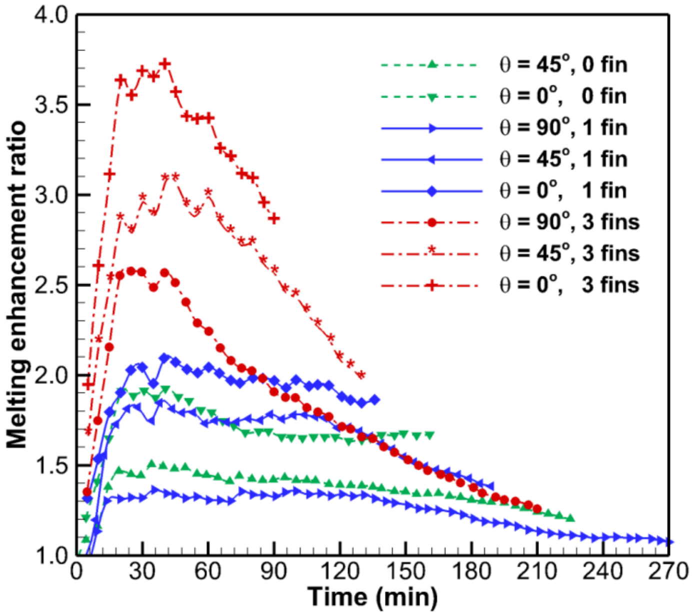

Figure 15. Melting enhancement ratios as a function of time for different inclination angles and number of fins (Figure reproduced from [79])

In the same line of thinking, Abdulmunem et al. [80] conducted experiments and numerical simulations to evaluate the paraffin wax PCM melting process as a passive cooling in a rectangular enclosure under different tilting angles (i.e. 0, 30, 60, and 90°). The geometry under consideration was subjected to 1000 sun simulator to maintain the temperature of an aluminum plate at 373 K. Figure 16 shows the liquid fraction time evolution in PCM charging process under various tilting angles. As seen in this figure, on contrary to other studies in the literature, the authors found that the melting time increased by lowering the tilting angle from 90° to 0°. They attributed this to lower convection heat transfer at lower inclination angle. In general, a shorter amount of time was needed for the PCM to completely melt, which indicates a more effective cooling performance. In another study, the authors focused on the charging performance of a PCM-based heat sink behind a rectangular domain of PV cells [81]. According to this analysis, the authors achieved 0.4% to 12% reduction in the PV cell temperature as a result of changing the tilting angle from 0° to 90° (see Figure 17). However, the authors did not assess the energy, exergy, and electrical efficiency of PV-PCM under different inclination angles.

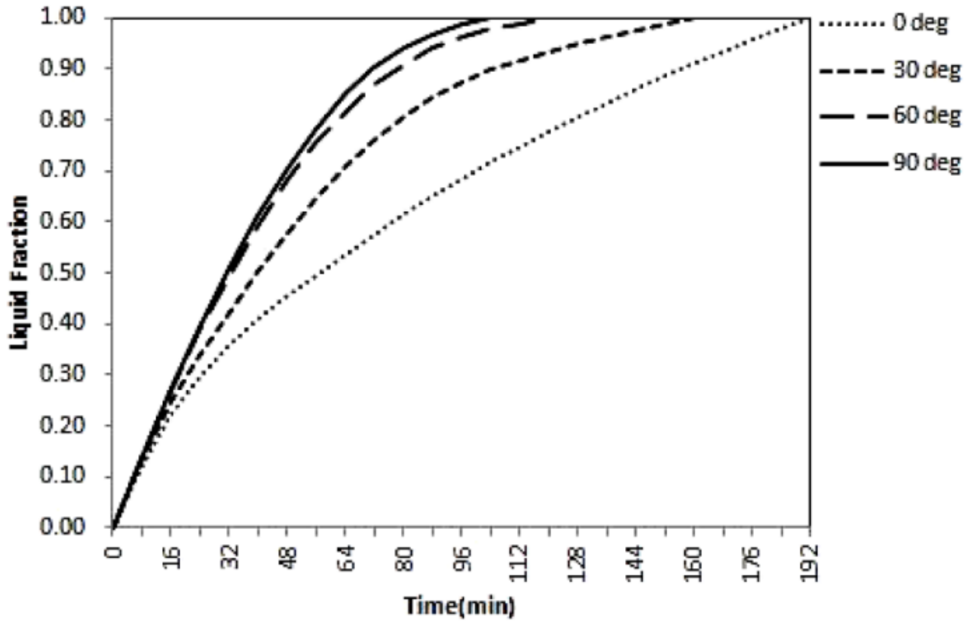

Figure 16. Liquid fraction time evolution in the charging process of PCM for various tilting angles (Figure reproduced from [80])

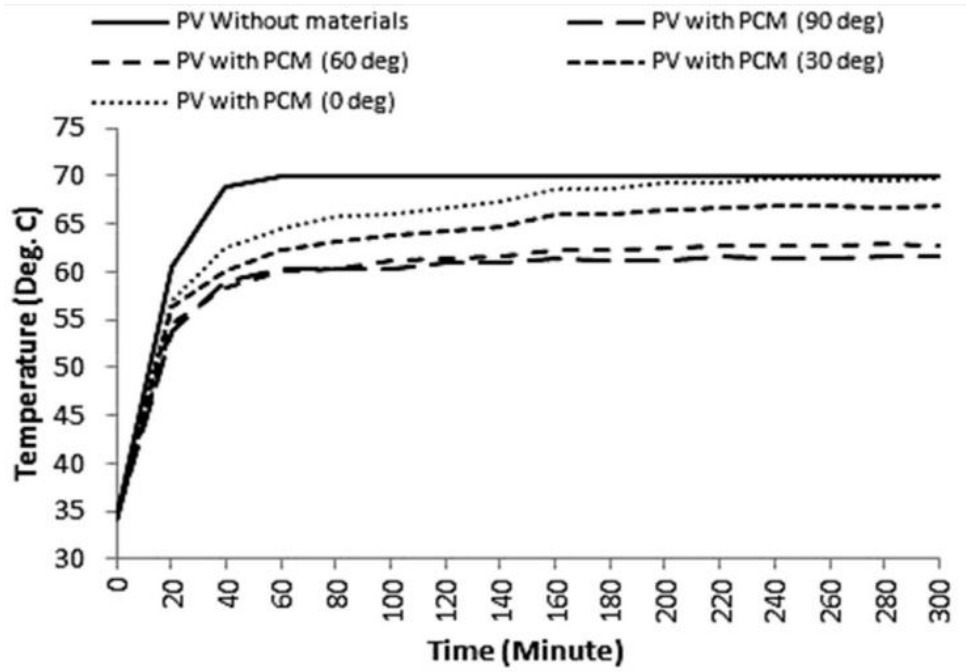

Figure 17. Variation of PV cell temperature with time for various tilting angles (Figure reproduced from [81])

5.3 Shell-and-tube heat exchanger

Kousha et al. [82] studies the melting and solidification performance of Paraffin RT35 PCM in a shell-and-tube heat exchanger under various inclination angles in the laminar flow regime.

The authors evaluated the effect of various parameters including Stefan number (i.e. 0.46, 0.52, and 0.58) and tilting angle ranging from 0° to 90°. Reynolds number was set at 770 and Grashof number was ranging from 4.6×10^4 to 5.8×10^4. They found that the increase in the inlet temperature was associated with faster melting process and lower melting time. The results showed that the melting/solidification rates were intensified in the horizontal/vertical orientation of the heat storage medium. Figure 18 shows the PCM temperature as a function of time during solidification for different tilting angles. As seen in this figure, there was a rapid reduction in the PCM temperature as a result of large temperature difference within the initial stage of the solidification process. The formation of solid PCM by progressing with time reduced the convection heat transfer by introducing the thermal resistance between the HTF and PCM. As a result, the conduction heat transfer was the more dominant mechanism during the solidification process. Regarding the effect of tilting angle, it was noticed that a LHTES system with 90° angle solidifies faster than other angles.

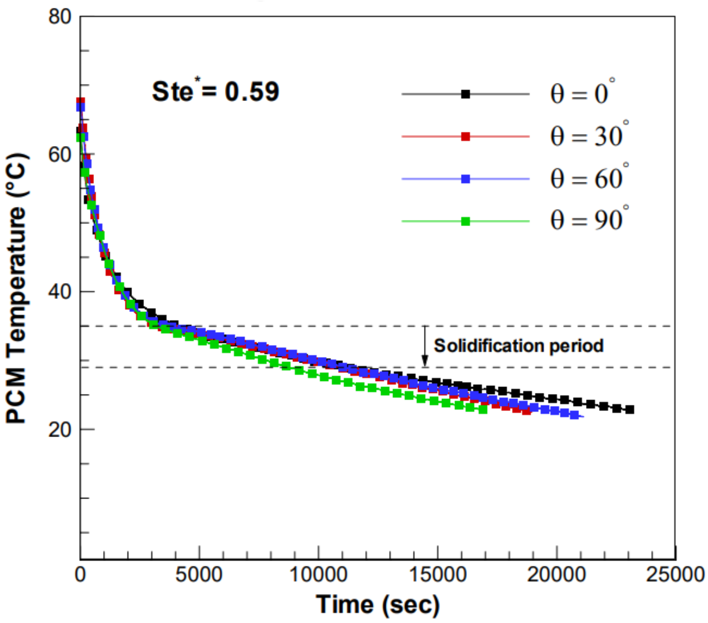

Figure 18. Variation of PCM temperature with time for different inclination angles (Figure reproduced from [82])

Shen et al. [83] developed a numerical model to evaluate the melting performance of a vertical shell-and-tube LHTES systems with variable tilting angles of the lateral surface. The results showed that increase in the tilting angle improved the heat transmission during the melting process while deteriorated the solidification performance. As a case in point, melting time shortened by 45% by increasing the angle from 0° to 7°. Figure 19 shows that the HTF temperature as a function of melting/solidification time. In case of the melting process, the

HTF outlet temperature was lower at higher tilting angle. This trend was then reversed when PCM starts the melting process due to the presence of more solid PCM in this case. In case of the solidification process, there was a marginal change in the HTF temperature with respect to the tilting angle. They also performed a detailed parametric study to find the optimum tilting angle of the lateral surface. According to their analysis, tilting angle of 4° was identified as the ideal angle—reducing the melting and solidification time by 22% and 8.5%.

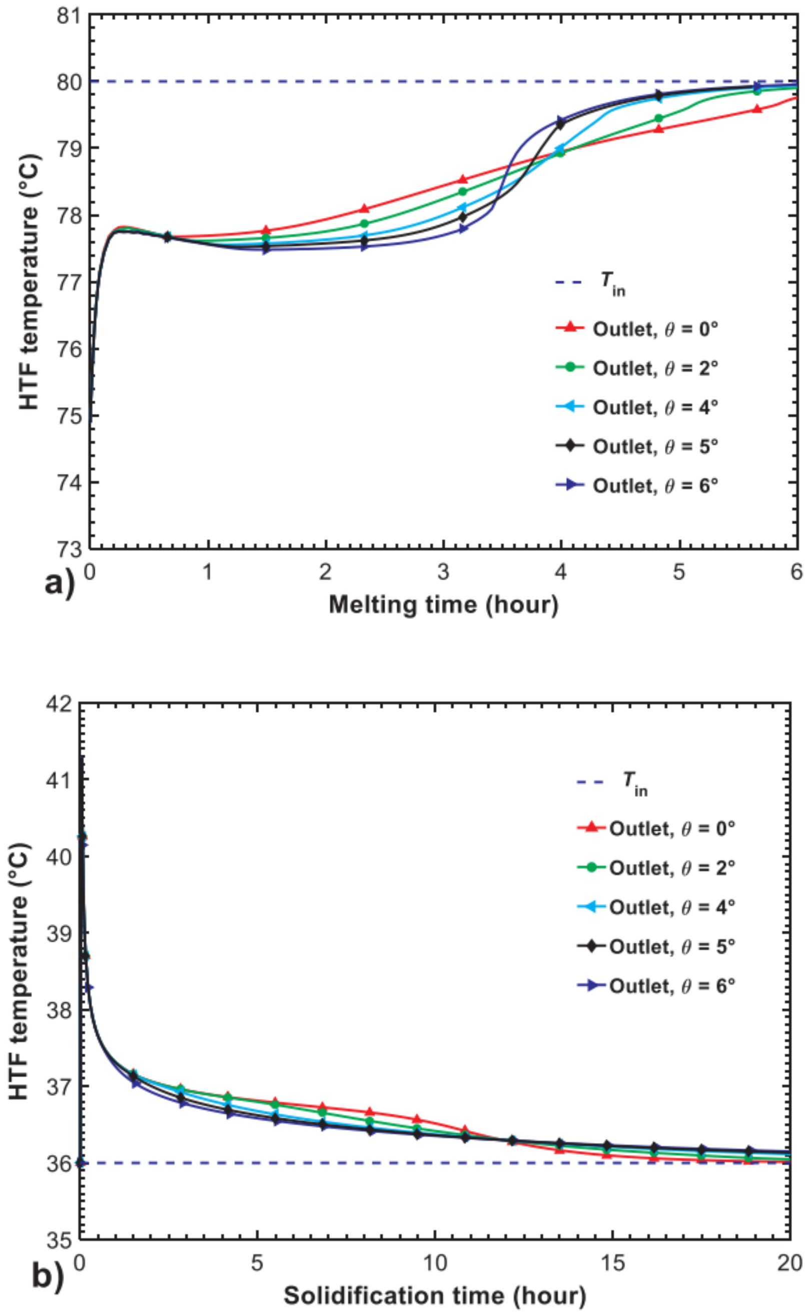

Figure 19. HTF outlet temperatures during (a) the melting and (b) solidification processes (Figure reproduced from [83])

5.4 Other geometries

Focusing on a flat-type heat sink, Avci and Yazici [84] assessed the melting performance of N-eicosane PCM under a range of inclination angles from 0° to 90°. An imaging technique was employed to observe the solid-liquid melting interface. The main finding of this work was an increase in the velocity of the melting front as a result of increasing the tilting angle—leading to a more uniform temperature distribution on the back side of the flat-type heat sink. However, this effect was insignificance in the without PCM case.

Karami and Kamkari [85] focused on the formation of convection flows in a finned cavities under different tilting angles (0° to 180°). They studied this effect for 3-fin and 1-fin rectangular cavities. The findings revealed that reducing the tilting angle shortened the melting duration due to more vortices and intensified natural convection in the liquid PCM. Figure 20 shows the heat transfer rate as a function of liquid fraction for various inclination angles and number of fins. The heat transfer rate was generally enhanced by increasing the number of fins at a constant tilting angle. In some specific cases, the results were not consistent shown by point F, G, and H. At point F, the heat transfer was higher for 1-fin case at 0° than 3-fin case at 90° beyond 0.56 liquid fraction. For points G and H, the rate of heat transfer in 1-fin case at 45° exceeds than 3-fin case at both 135° and 180°.

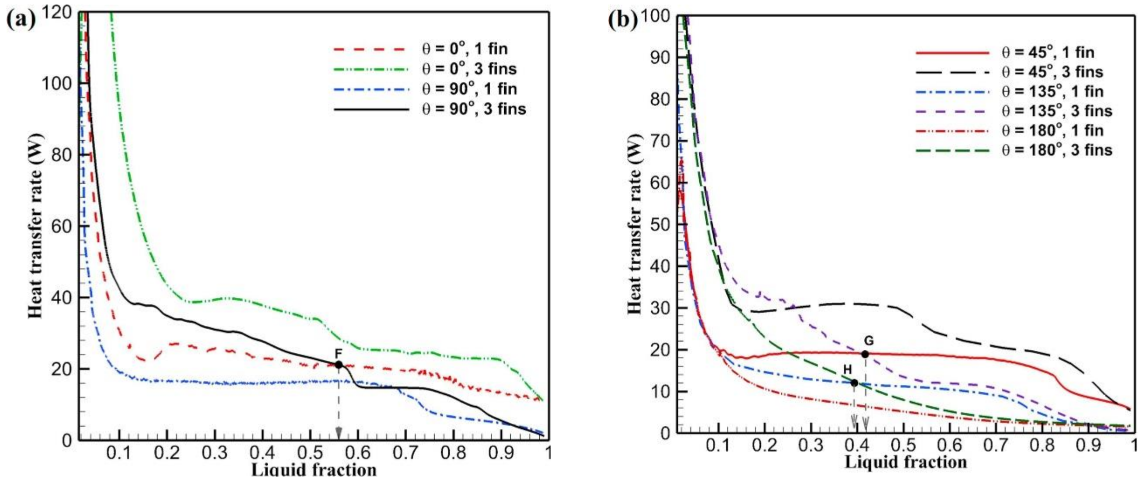

Figure 20. Variation of heat transfer rate with liquid fraction for various tilting angles and number of fins (Figure reproduced from [85])

Ghalambaz et al. [86] investigated the charging process of octadecane NEPCM with mesoporous silica particles in an inclined enclosure. The phase-change boundary and heat transmission in the enclosure were tracked using a deformed mesh model. The Arbitrary Lagrangian-Eulerian moving mesh approach and finite element method were used to solve the phase-change equations. Figure 21 shows the NMVF and average Nusselt number versus

Fourier number for various tilting angles. Regarding the role of tilting angle, the authors found that heat transfer was reduced by 80% at -75° tilting angle. This was due to the hinderance in the convection flows and less melting at higher tilting angles. This was also evident in the average Nusselt number, a significant reduction at -75° angle as a result of lower heat transfer. With respect to nanoparticle addition, the results showed lower phase change heat transfer by adding nanoparticles. This was attributed to a higher viscosity of the liquid, which prevents the natural convection flow. As a case in point, employing 5% nanoparticles reduced the heat transfer by 50%.

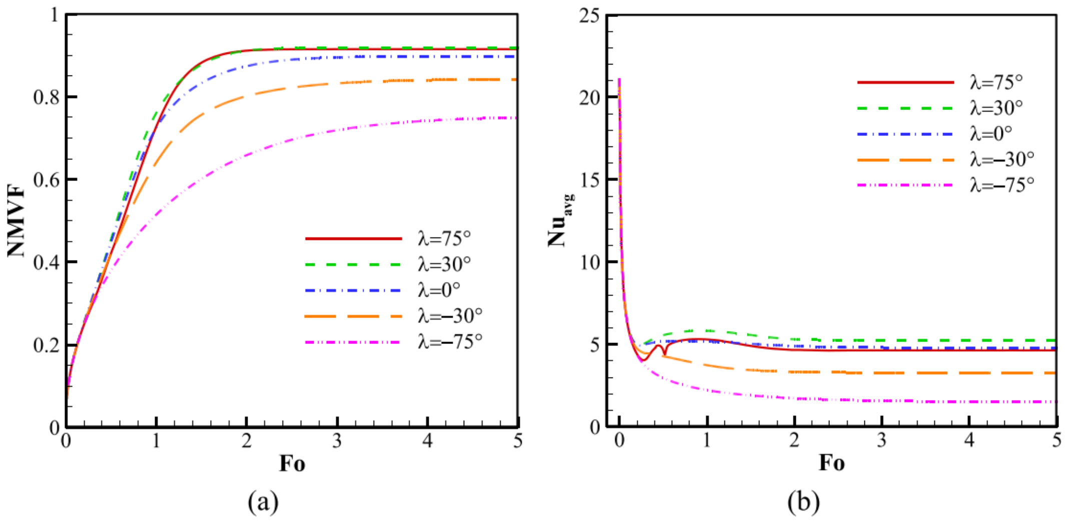

Figure 21. Variation of NMVF and average Nusselt number versus Fourier number for various tilting angles (Figure reproduced from [86])

Sorour et al. [87] studied the PCM melting in a double-pipe LHTES system with hot water flowing in the inner tube and PCM located in the annulus. They performed a detailed parametric study over the PCM mass (i.e. 0.154, 0.308, and 0.46 kg), PCM thickness (i.e. 7, 11.28, and 14.5 mm), and LHTES tilting angles (i.e. 0°, 15°, 30°, 45°, 60°, 75°, and 90°). Depending on the thickness of PCM, the tilting angle showed different effects on the melting process. Figure 22 shows the variation of melting time with inclination angle for various thickness of PCM. As seen in this figure, PCM with 7 mm thickness experiences the lowest duration of melting. However, switching to PCM thickness of 11.28, and 14.5 mm increased the optimum tilting angle to 45°. The proposed system had the highest melting time at 90° angle regardless of the PCM thickness.

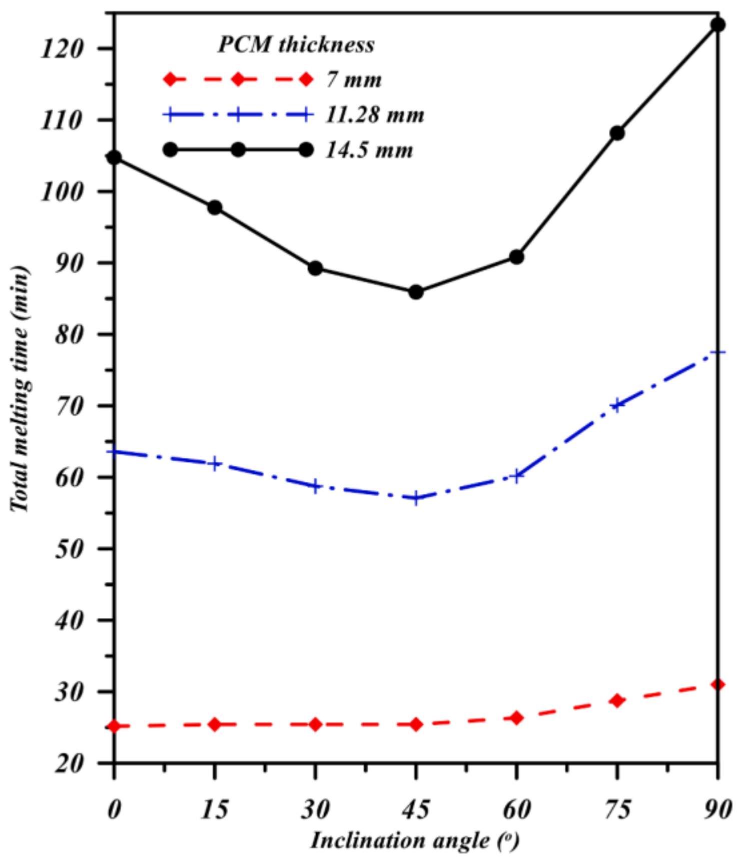

Figure 22. Variation of melting time with inclination angle for various thickness of PCM (Figure reproduced from [87])

Following the same research direction, Kothari et al. [88] focused on Paraffin wax PCM melting in the heat sink with/without plate fins. The authors examined different heat flux values (i.e. 1.3, 2.0, and 2.7 kW/m^2) and inclination angles (i.e. 0^o to 90^o with 15° interval). Figure 23 shows the variation melting time with inclination angle for unfinned and finned PCM-based heat sinks. As seen in this figure, the lowest melting time was achieved in three-finned cases for all the inclination angles. It was found that the inclination angle of 0° was the optimum melting angle compared to other cases as a result of more circulation current in the liquid PCM—reducing the time by 44% and 30% for unfinned and finned configurations. It should be noted that there is an optimum fin number, beyond which there is no further reduction in the melting time due to the impediment in the convection flow of liquid PCM.

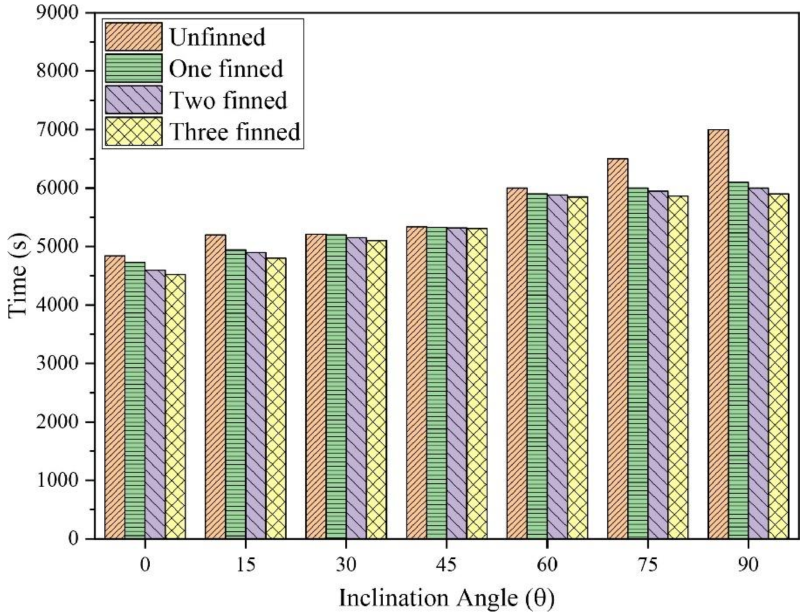

Figure 23. Variation of melting time with inclination angle for unfinned and finned PCM-based heat sinks (Figure reproduced from [88])

Yang et al. [89] conducted a numerical and experimental study on the melting process of PCM with metal foam in a cavity with various aspect ratios, defined as the width to height ratio of the cavity. They analysed the melting rate, phase interface, flow streamline, heat storage capacity, temperature distribution, and heat transfer performance. Figure 24 shows the variation of heat storage capacity with melting time for composite PCM at various aspect ratios of the enclosure and tilting angles of a heating surface. The results indicated that at a constant aspect ratio, the inclination of the heating surface had a negligible impact on the melting rate and heat storage capacity. However, the geometry with the aspect ratio of 0.1 experienced a better temperature uniformity and higher heat storage capacity in a shorter period of time.

Wang et al. [89] investigated the charging process of flat heat pipe LHTES unit under various tilting angles. They designed a LHTES unit using flat heat pipe and lauric acid with adjustable angles. The results showed a delayed melting time of the PCM at lower inclination angle even though the heat transfer was improved on the PCM side. They also noticed a decreasing and then increasing trend in the thermal conductivity when the tilting angle increased from 30° to 90°. The feasibility analysis showed that heat transfer was deteriorated at higher power input of 30 W under low inclination angle of below 30°.

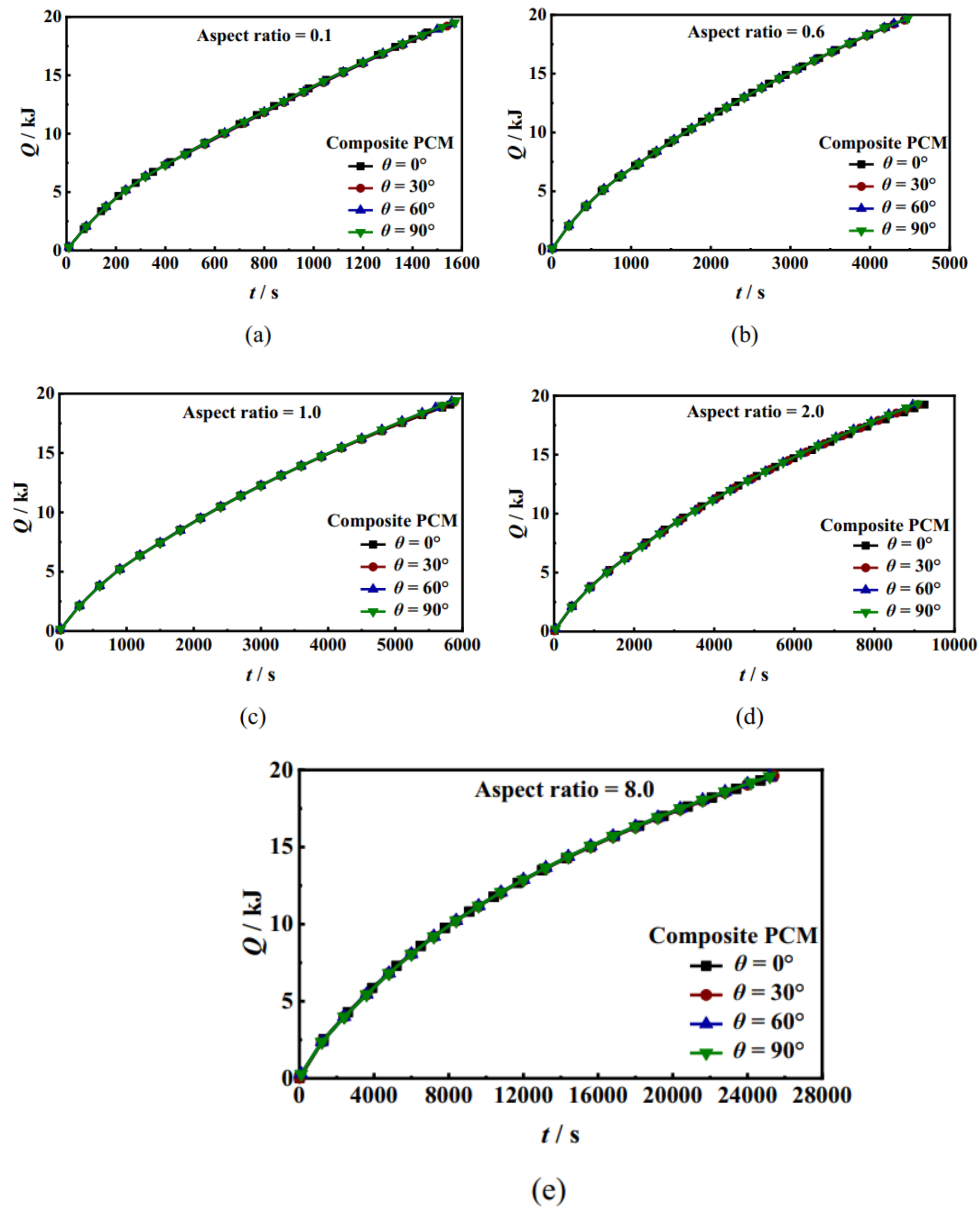

Figure 24. Variation of heat storage capacity with melting time for composite PCM at various aspect ratios of the enclosure and tilting angles of a heating surface (Figure reproduced from [89])

6. Effect of vibration

Vibration and oscillation have been used in several studies to improve heat and mass transfer in tubular laminar flow. Tubular laminar flow is often used in various energy transport systems, including chemical reactions, thermal sterilizing, slurry flow, and the industries of food and pharmaceuticals. Table 4 lists the geometrical, operating conditions, and key take-away findings of recent studies addressing the role vibration on the melting/solidification procedures of PCMs/NEPCMs inside an enclosure with different geometries. The citation list [91–94] focuses on this importance in different geometries as summarized in the following subsections.

Table 4. A summary of studies on the effect of vibration on the melting/solidification procedures of PCMs/NEPCMs inside an enclosure with different geometries

Authors (year)	**Configuration**	**Type of study**	**Studied parameters**	**Highlighted results/findings**
Hajiyan et al. (2018) [91]	PCM placed in a cylindrical geometry	Numerical	Effect of vibration on the melting process	Different melting behavior in the presence of vibration force. No stratification observed as a result of vibration force, leading to equal melting rate at the bottom/top of the enclosure.
Joshy et al. (2020) [92]	PCM-based thermal management of electric vehicle Lithium-ion battery cells	Experimental	Effect of frequency and amplitude vibration on the solidification process	Frequency as the most dominant parameter on the temperature rise at low discharge rate. Amplitude and frequency as significant factors at high discharge rate Lower temperature at the outer edges of the battery surface in a staggered arrangement of batteries.
Vadasz et al. (2012) [93]	RT35 PCM embedded in a spherical shell under vibration effect	Experimental	Effect of vibration on the solidification process	Shorter solidification time when PCM was subjected to vibration More uniform solid structure at higher vibration frequency.
Zhou et al. (2018) [94]	Super-cooled sodium acetate PCM inside a rounded-rectangular enclosure vibrated through freely falling steel ball solution was cooled to very low temperatures.	Experimental and numerical	Effect of falling height, steel ball diameter, and percussion position on the solidification process	Better solidification performance under larger striking momentum Effective commencement of the solidification process with percussion momentum imposed near the edges or cover lid.

6.1 Cylindrical geometry

Hajiyan et al. [91] numerically studied the PCM charging inside a cylindrical container subjected to vibration effect. The phase transition of PCM was modeled using enthalpy-porosity method, applicable for convection-diffusion phase change during the melting process of a pure metal. To simulate the charging behavior of a PCM under vibrational circumstances, the COMSOL Multiphysics program was used. According to their findings, the behavior of the melting process is greatly impacted by vibration.

Joshy et al. [92] investigated the influence of vibration on battery thermal management (BTM) system embedded with PCM. Aluminum cylinders with ceramic cartridge heaters replicated the Lithium-ion batteries. The amplitude and frequency were varied from 30–50 mm/s and 20–30 Hz, as typical values for hybrid electric vehicles (PHEV). Figure 25 shows the variation of temperature at the selected battery surface (T1 cell location in this case) with time for various discharge rate. According to this figure, the battery temperature increased with the vibration frequency for both cases. It should be noted that this effect was not significant when the temperature was below the PCM melting point. The liquid motion as a result of buoyancy effect helped with the formation of thermal boundary layer—leading to the expansion of liquid region at the top by thermal stratification effect in the no vibration case. However, the addition of vibration may help or deteriorate the gravitational force, which may assist or hinder the movement of liquid phase and natural convection flows.

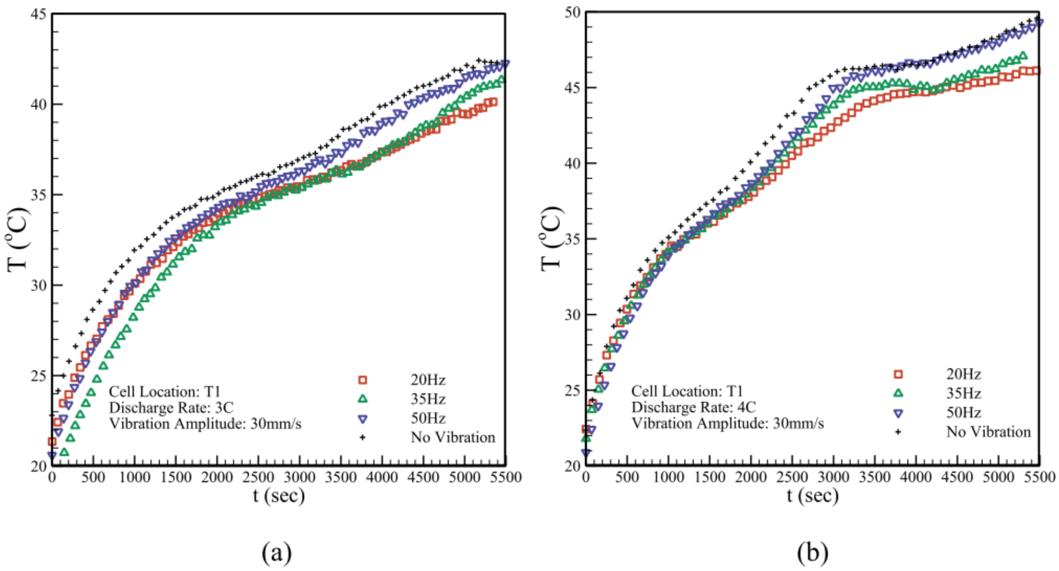

Figure 25. Variation of temperature at the selected battery surface (T1 cell location in this case) with time for 30 mm/s amplitude: (a) 3C discharge rate and (b) 4C discharge rate (Figure reproduced from [92])

6.2 Other geometries

Vadasz et al. [93] evaluated the impacts of vibration on the discharging procedure of paraffin wax PCM in a spherical shell. Experiments were carried out on a sphere with a diameter of 40 mm and wall temperature of 20°C lower than the mean solidification temperature. The setup was exposed to a vibration frequency ranging from 10 to 300 Hz. The authors compared the results with no vibration case. An improvement in heat transmission through the use of vibration decreased the amount of time required for discharging the heat from PCM. Zhou et al. [94] conducted a series of tests in a thermal storage unit of rounded-rectangular geometry to investigate the effect of percussive vibration on triggering the discharging of salt solution of super-cooled sodium acetate. The steel ball was allowed to freely fall to the PCM surface unit, which was then subjected to percussion vibration using the parameters of crystallization induction time and percussion number. According to the findings, it was best to activate the discharging of the super-cooled sodium acetate solution using a percussion with a greater momentum (a larger ball diameter and a higher falling height).

7. Conclusions

Given the intermittency nature of renewable energy resources, the development of fast-responsive and low-cost thermal energy storage (TES) technologies are of vital importance. However, latent heat thermal energy storage (LHTES) systems filled with phase change materials (PCMs) often suffer from low heat transfer rates. Previous studies have primarily focused on using fins and novel encapsulated PCMs (NEPCMs) as methods of enhancing heat transfer. This paper aimed to provide a comprehensive review of the effect of other factors, including the application of a magnetic field, rotation, tilt angle, and vibration, on the melting and solidification performance of PCMs inside enclosures with various geometries.

It was found that increasing the magnetic number and decreasing the Hartmann number are important to accelerate the melting and solidification processes of phase change materials (PCMs) used in thermal energy storage (TES) systems. The direction of the magnetic field showed marginal influence on the charging/discharging processes. A dual non-uniform magnetic fields might have potential design and operational implications for PCM-TES systems to enhance the heat transfer and improve the overall performance of TES systems.

Another design parameter was the rotation of LHTES unit. Reviewing the literature revealed that rotating the enclosure in a counter direction of buoyancy flow improved the melting rate/time. A possible method to greatly minimise the melting time was to use dual opposing rotations with a 180° difference between the stop ends. In case of intermittent rotation, an increase in bottom eccentricity was found to enhance the melting process, while an increase in top eccentricity resulted in an improvement of the solidification process.

In terms of tilting angle effect, the maximum melting rate was achieved in the horizontal orientation of the enclosure for PCMs with a small thickness. However, it was shown that switching to sufficiently thicker PCM can increase the optimum tilting angle. Increasing the tilting lateral surface angle of the cavity improved and deteriorated the charging and discharging processes.

Even though vibration was identified as an effective approach to enhance the heat transfer in LHTES unit, only a very few studies have focused on the performance of PCM under vibration frequency. Taken together, it was found that frequency and amplitude/frequency were the significant factors at low and high discharge rates, respectively. The percussion momentum and strength are effective parameters to trigger the melting/solidification processes.

There are some interesting unanswered questions arising from the review of previously published studies in this realm including: (i) the interaction between several active and passive methods in terms of improving the melting and solidification processes, (ii) the determination of optimum design parameters leading to maximum heat transfer during the charging/discharging cycles, (iii) the use of machine learning algorithms together with CFD to predict the thermal performance of PCMs under different operating conditions, and (iv) the technical challenges and economic aspects of the proposed techniques.

References

1. Akeiber, H., et al., *A review on phase change material (PCM) for sustainable passive cooling in building envelopes.* Renewable and Sustainable Energy Reviews, 2016. **60**: p. 1470-1497.
2. Dhaidan, N.S., et al., *Review of solidification of phase change materials dispersed with nanoparticles in different containers.* Journal of Energy Storage, 2022. **51**: p. 104271.
3. Rashid, F.L., et al., *Review of Heat Transfer Analysis in Different Cavity Geometries with and without Nanofluids.* Nanomaterials, 2022. **12**(14): p. 2481.
4. Baetens, R., B.P. Jelle, and A. Gustavsen, *Phase change materials for building applications: A state-of-the-art review.* Energy and Buildings, 2010. **42**(9): p. 1361-1368.
5. Tiji, M.E., et al., *Thermal Management of the Melting Process in a Latent Heat Triplex Tube Storage System Using Different Configurations of Frustum Tubes.* Journal of Nanomaterials, 2022. **2022**: p. 7398110.
6. Mohammed, H.I., *Discharge improvement of a phase change material-air-based thermal energy storage unit for space heating applications using metal foams in the air sides.* Heat Transfer, 2022. **51**(5): p. 3830-3852.
7. Sheikholeslami, M., et al., *Simulation of nanoparticles application for expediting melting of PCM inside a finned enclosure.* Physica A: Statistical Mechanics and its Applications, 2019. **523**: p. 544-556.
8. Sheikholeslami, M. and O. Mahian, *Enhancement of PCM solidification using inorganic nanoparticles and an external magnetic field with application in energy storage systems.* Journal of Cleaner Production, 2019. **215**: p. 963-977.
9. Sheikholeslami, M., et al., *Heat transfer simulation of heat storage unit with nanoparticles and fins through a heat exchanger.* International Journal of Heat and Mass Transfer, 2019. **135**: p. 470-478.
10. Sheikholeslami, M., et al., *Heat transfer behavior of nanoparticle enhanced PCM solidification through an enclosure with V shaped fins.* International Journal of Heat and Mass Transfer, 2019. **130**: p. 1322-1342.
11. Nóbrega, C.R.E.S., K.A.R. Ismail, and F.A.M. Lino, *Solidification around axial finned tube submersed in PCM: Modeling and experiments.* Journal of Energy Storage, 2020. **29**: p. 101438.
12. Khademi, A., et al., *A brief review on different hybrid methods of enhancement within latent heat storage systems.* Journal of Energy Storage, 2022. **54**: p. 105362.
13. Bergles, A.E., *Recent developments in enhanced heat transfer.* Heat and Mass Transfer, 2011. **47**(8): p. 1001.
14. Sharma, S.D. and K. Sagara, *Latent Heat Storage Materials and Systems: A Review.* International Journal of Green Energy, 2005. **2**(1): p. 1-56.

15. Joybari, M.M., et al., *Heat transfer enhancement of phase change materials by fins under simultaneous charging and discharging.* Energy Conversion and Management, 2017. **152**: p. 136-156.
16. Abed, A.M., et al., *Numerical analysis of the energy-storage performance of a PCM-based triplex-tube containment system equipped with arc-shaped fins.* Frontiers in Chemistry, 2022. **10**.
17. Chen, K., et al., *Effects of non-uniform fin arrangement and size on the thermal response of a vertical latent heat triple-tube heat exchanger.* Journal of Energy Storage, 2022. **45**: p. 103723.
18. Ebrahimnataj Tiji, M., et al., *Evaluation of T-Shaped Fins With a Novel Layout for Improved Melting in a Triple-Tube Heat Storage System.* 2022.
19. Sun, X., et al., *Investigation of Heat Transfer Enhancement in a Triple Tube Latent Heat Storage System Using Circular Fins with Inline and Staggered Arrangements.* Nanomaterials, 2021. **11**(10): p. 2647.
20. Agyenim, F., P. Eames, and M. Smyth, *A comparison of heat transfer enhancement in a medium temperature thermal energy storage heat exchanger using fins.* Solar Energy, 2009. **83**(9): p. 1509-1520.
21. Mahmoud, M.Z., et al., *Melting Enhancement in a Triple-Tube Latent Heat Storage System with Sloped Fins.* Nanomaterials, 2021. **11**(11): p. 3153.
22. Ji, C., et al., *Non-uniform heat transfer suppression to enhance PCM melting by angled fins.* Applied Thermal Engineering, 2018. **129**: p. 269-279.
23. Ghalambaz, M., et al., *Intensifying the Charging Response of a Phase-Change Material with Twisted Fin Arrays in a Shell-And-Tube Storage System.* Energies, 2021. **14**(6): p. 1619.
24. Yıldız, Ç., et al., *Numerical investigation of natural convection behavior of molten PCM in an enclosure having rectangular and tree-like branching fins.* Energy, 2020. **207**: p. 118223.
25. Liu, X., et al., *An experimental investigation on the rheological behavior of nanofluids made by suspending multi-walled carbon nanotubes in liquid paraffin.* Journal of Molecular Liquids, 2020. **300**: p. 112269.
26. Ju, Y., et al., *Evaluation of Multiple Semi-Twisted Tape Inserts in a Heat Exchanger Pipe Using Al2O3 Nanofluid.* Nanomaterials, 2021. **11**(6): p. 1570.
27. Eisapour, M., et al., *Solidification of a nano-enhanced phase change material (NePCM) in a double elliptical latent heat storage unit with wavy inner tubes.* Solar Energy, 2022. **241**: p. 39-53.
28. Al-Jethelah, M., et al., *Nano-PCM filled energy storage system for solar-thermal applications.* Renewable Energy, 2018. **126**: p. 137-155.
29. Ebadi, S., et al., *Melting of nano-PCM inside a cylindrical thermal energy storage system: Numerical study with experimental verification.* Energy Conversion and Management, 2018. **166**: p. 241-259.
30. Gorzin, M., et al., *Nano-enhancement of phase change material in a shell and multi-PCM-tube heat exchanger.* Journal of Energy Storage, 2019. **22**: p. 88-97.
31. Bashar, M. and K. Siddiqui, *Experimental investigation of transient melting and heat transfer behavior of nanoparticle-enriched PCM in a rectangular enclosure.* Journal of Energy Storage, 2018. **18**: p. 485-497.
32. Shastry, D.M.C. and U.C. Arunachala, *Thermal management of photovoltaic module with metal matrix embedded PCM.* Journal of Energy Storage, 2020. **28**: p. 101312.
33. Mahdi, J.M., et al., *Simultaneous and consecutive charging and discharging of a PCM-based domestic air heater with metal foam.* Applied Thermal Engineering, 2021. **197**: p. 117408.

34. Sardari, P.T., et al., *Numerical study of a multiple-segment metal foam-PCM latent heat storage unit: Effect of porosity, pore density and location of heat source.* Energy, 2019. **189**: p. 116108.
35. Kumar, A. and S.K. Saha, *Latent heat thermal storage with variable porosity metal matrix: A numerical study.* Renewable Energy, 2018. **125**: p. 962-973.
36. Tiji, M.E., et al., *Natural Convection Effect on Solidification Enhancement in a Multi-Tube Latent Heat Storage System: Effect of Tubes' Arrangement.* Energies, 2021. **14**(22): p. 7489.
37. Ghalambaz, M., et al., *Impact of Tube Bundle Placement on the Thermal Charging of a Latent Heat Storage Unit.* Energies, 2021. **14**(5): p. 1289.
38. Ghalambaz, M., et al., *Optimum Placement of Heating Tubes in a Multi-Tube Latent Heat Thermal Energy Storage.* Materials, 2021. **14**(5): p. 1232.
39. Talebizadehsardari, P., et al., *Consecutive charging and discharging of a PCM-based plate heat exchanger with zigzag configuration.* Applied Thermal Engineering, 2021. **193**: p. 116970.
40. Mahani, R.B., et al. *Phase Change Process in a Zigzag Plate Latent Heat Storage System during Melting and Solidification*. Molecules, 2020. **25**, DOI: 10.3390/molecules25204643.
41. Eisapour, A.H., et al., *A new design to enhance the conductive and convective heat transfer of latent heat thermal energy storage units.* Applied Thermal Engineering, 2022. **215**: p. 118955.
42. Eisapour, A.H., et al., *Optimum design of a double elliptical latent heat energy storage system during the melting process.* Journal of Energy Storage, 2021. **44**: p. 103384.
43. Shi, J., et al., *Review of phase change heat transfer enhancement by metal foam.* Applied Thermal Engineering, 2023. **219**: p. 119427.
44. Nematpour Keshteli, A. and M. Sheikholeslami, *Nanoparticle enhanced PCM applications for intensification of thermal performance in building: A review.* Journal of Molecular Liquids, 2019. **274**: p. 516-533.
45. Teggar, M., et al., *Performance enhancement of latent heat storage systems by using extended surfaces and porous materials: A state-of-the-art review.* Journal of Energy Storage, 2021. **44**: p. 103340.
46. Ghosh, Debasree, Joyjeet Ghose, Pulak Datta, Pallavi Kumari, and Suraj Paul, *Strategies for phase change material application in latent heat thermal energy storage enhancement: Status and prospect*. Journal of Energy Storage, 2022. **53**: p. 105179.
47. Lei, S., Y. Chen, and L. Jia, *Directional Solidification of Graphene/Paraffin Nanofluids Assisted by Electromagnetic Field.* Energy Procedia, 2015. **75**: p. 3290-3294.
48. Laouer, A., et al., *Effect of Magnetic Field and Nanoparticle Concentration on Melting of Cu-Ice in a Rectangular Cavity under Fluctuating Temperatures.* Journal of Energy Storage, 2021. **36**: p. 102421.
49. Fan, Y., et al., *Melting performance enhancement of phase change material with magnetic particles under rotating magnetic field.* Journal of Energy Storage, 2021. **38**: p. 102540.
50. Farahani, S.D., et al., *Control of PCM melting process in an annular space via continuous or discontinuous fin and non-uniform magnetic field.* Journal of Energy Storage, 2022. **55**: p. 105410.
51. Farahani, S.D., et al., *The effect of novel fin shapes and non-uniform magnetic field on the nanoparticles embedded PCM melting in a tube.* Journal of Magnetism and Magnetic Materials, 2022. **562**: p. 169826.

52. Saha, S.K., *Dynamics of phase change of gallium under magnetic field and thermocapillary effects under variable gravity conditions.* Thermal Science and Engineering Progress, 2022. **29**: p. 101234.
53. Selimefendigil, F. and H.F. Öztop, *Combined effects of bifurcation and magnetic field on the performance of phase change material installed cylinder with small inlet temperature perturbations during nanofluid convection.* International Journal of Heat and Mass Transfer, 2022. **188**: p. 122640.
54. Kohyani, M.T., et al., *Melting of cyclohexane–Cu nano-phase change material (nano-PCM) in porous medium under magnetic field.* Journal of the Taiwan Institute of Chemical Engineers, 2017. **77**: p. 142-151.
55. Ghalambaz, M., et al., *Non-Newtonian behavior of an electrical and magnetizable phase change material in a filled enclosure in the presence of a non-uniform magnetic field.* International Communications in Heat and Mass Transfer, 2020. **110**: p. 104437.
56. Mehryan, S.A.M., et al., *Melting behavior of phase change materials in the presence of a non-uniform magnetic-field due to two variable magnetic sources.* International Journal of Heat and Mass Transfer, 2020. **149**: p. 119184.
57. Kumar, A., et al., *Study of melting of paraffin dispersed with copper nanoparticles in square cavity subjected to external magnetic field.* Journal of Energy Storage, 2022. **50**: p. 104338.
58. Rostami Dibavar, M., et al., *Numerical study on the effect of non-uniform magnetic fields on melting and solidification characteristics of NEPCMs in an annulus enclosure.* Energy Conversion and Management, 2018. **171**: p. 879-889.
59. Sheikholeslami, M., *Solidification of NEPCM under the effect of magnetic field in a porous thermal energy storage enclosure using CuO nanoparticles.* Journal of Molecular Liquids, 2018. **263**: p. 303-315.
60. Ghalambaz, M., et al., *Analysis of melting behavior of PCMs in a cavity subject to a non-uniform magnetic field using a moving grid technique.* Applied Mathematical Modelling, 2020. **77**: p. 1936-1953.
61. Shi, E., et al., *Enhancement of the performance of a NEPCM filled shell-and-multi tube thermal energy storage system using magnetic field: A numerical study.* Applied Thermal Engineering, 2020. **178**: p. 115604.
62. Selimefendigil, F. and H.F. Öztop, *Impacts of magnetic field and hybrid nanoparticles in the heat transfer fluid on the thermal performance of phase change material installed energy storage system and predictive modeling with artificial neural networks.* Journal of Energy Storage, 2020. **32**: p. 101793.
63. Fan, Y., et al., *Performance enhancement of latent thermal energy system under alternating magnetic field.* Applied Thermal Engineering, 2021. **188**: p. 116586.
64. He, W., et al., *Thermo-magnetic convection regulating the solidification behavior and energy storage of Fe3O4 nanoparticles composited paraffin wax under the magnetic-field.* Applied Thermal Engineering, 2022. **214**: p. 118617.
65. Aly, A.M., et al., *Thermal diffusion upon magnetic field convection of nano-enhanced phase change materials in a permeable wavy cavity with crescent-shaped partitions.* Case Studies in Thermal Engineering, 2022. **31**: p. 101855.
66. Jaberi Khosroshahi, A. and S. Hossainpour, *Investigation of storage rotation effect on phase change material charging process in latent heat thermal energy storage system.* Journal of Energy Storage, 2021. **36**: p. 102442.
67. Jaberi khosroshahi, A. and S. Hossainpour, *A numerical investigation on the finned storage rotation effect on the phase change material melting process of latent heat thermal energy storage system.* Journal of Energy Storage, 2022. **55**: p. 105461.

68. Fathi, M.I. and M.A. Mussa, *Experimental study on the effect of tube rotation on performance of horizontal shell and tube latent heat energy storage.* Journal of Energy Storage, 2021. **39**: p. 102626.
69. Soltani, H., et al., *Heat transfer enhancement in latent heat thermal energy storage unit using a combination of fins and rotational mechanisms.* International Journal of Heat and Mass Transfer, 2021. **179**: p. 121667.
70. Modi, N., X. Wang, and M. Negnevitsky, *Melting and solidification characteristics of a semi-rotational eccentric tube horizontal latent heat thermal energy storage.* Applied Thermal Engineering, 2022. **214**: p. 118812.
71. Yang, C., et al., *Experimental study on the effect of rotation on melting performance of shell-and-tube latent heat thermal energy storage unit.* Applied Thermal Engineering, 2022. **215**: p. 118877.
72. Farsani, R.Y., et al., *Melting characteristics of paraffin wax in a rectangular cavity under steady rotations.* Journal of the Taiwan Institute of Chemical Engineers, 2020. **113**: p. 135-141.
73. Alhashash, A. and H. Saleh, *Free convection flow of a heterogeneous mixture of water and nano-encapsulated phase change particle (NEPCP) in enclosure subject to rotation.* Journal of Energy Storage, 2022. **51**: p. 104168.
74. Sharifi, N., et al., *Three-dimensional PCM melting in a vertical cylindrical enclosure including the effects of tilting.* International Journal of Heat and Mass Transfer, 2013. **65**: p. 798-806.
75. Allen, M.J., et al., *Effect of inclination angle during melting and solidification of a phase change material using a combined heat pipe-metal foam or foil configuration.* International Journal of Heat and Mass Transfer, 2015. **80**: p. 767-780.
76. Al Siyabi, I., et al., *An experimental and numerical study on the effect of inclination angle of phase change materials thermal energy storage system.* Journal of Energy Storage, 2019. **23**: p. 57-68.
77. Zennouhi, H., et al., *Effect of inclination angle on the melting process of phase change material.* Case Studies in Thermal Engineering, 2017. **9**: p. 47-54.
78. Joneidi, M.H., et al., *Experimental investigation of phase change in a cavity for varying heat flux and inclination angles.* Experimental Thermal and Fluid Science, 2017. **88**: p. 594-607.
79. Kamkari, B. and D. Groulx, *Experimental investigation of melting behaviour of phase change material in finned rectangular enclosures under different inclination angles.* Experimental Thermal and Fluid Science, 2018. **97**: p. 94-108.
80. Abdulmunem, A.R., et al., *Experimental and numerical investigations on the effects of different tilt angles on the phase change material melting process in a rectangular container.* Journal of Energy Storage, 2020. **32**: p. 101914.
81. Abdulmunem, A.R., et al., *Numerical and experimental analysis of the tilt angle's effects on the characteristics of the melting process of PCM-based as PV cell's backside heat sink.* Renewable Energy, 2021. **173**: p. 520-530.
82. Kousha, N., et al., *Effect of inclination angle on the performance of a shell and tube heat storage unit – An experimental study.* Applied Thermal Engineering, 2017. **112**: p. 1497-1509.
83. Shen, G., et al., *Study of the effect of tilting lateral surface angle and operating parameters on the performance of a vertical shell-and-tube latent heat energy storage system.* Solar Energy, 2019. **194**: p. 103-113.
84. Avci, M. and M.Y. Yazici, *An experimental study on effect of inclination angle on the performance of a PCM-based flat-type heat sink.* Applied Thermal Engineering, 2018. **131**: p. 806-814.

85. Karami, R. and B. Kamkari, *Investigation of the effect of inclination angle on the melting enhancement of phase change material in finned latent heat thermal storage units.* Applied Thermal Engineering, 2019. **146**: p. 45-60.
86. Ghalambaz, M., et al., *Non-Newtonian phase-change heat transfer of nano-enhanced octadecane with mesoporous silica particles in a tilted enclosure using a deformed mesh technique.* Applied Mathematical Modelling, 2020. **85**: p. 318-337.
87. Sorour, M.M., et al., *The effect of inclination angle on the performance characteristic of a double-pipe latent heat storage unit.* Journal of Energy Storage, 2021. **34**: p. 102202.
88. Kothari, R., et al., *Experimental investigation of the effect of inclination angle on the performance of phase change material based finned heat sink.* Journal of Energy Storage, 2021. **37**: p. 102462.
89. Yang, X., et al., *Influence of aspect ratios for a tilted cavity on the melting heat transfer of phase change materials embedded in metal foam.* International Communications in Heat and Mass Transfer, 2021. **122**: p. 105127.
90. Wang, Z., et al., *Effect of inclination angle on the charging process of flat heat pipe-assisted latent heat storage unit.* Journal of Energy Storage, 2022. **51**: p. 104402.
91. Hajiyan, M., et al., *Effect of Vibration on the Melting of Phase Change Material inside a Cylindrical Enclosure.* Proceedings of the 5th International Conference of Fluid Flow, Heat and Mass Transfer (FFHMT'18), 2018.
92. Joshy, N., et al., *Experimental investigation of the effect of vibration on phase change material (PCM) based battery thermal management system.* Journal of Power Sources, 2020. **450**: p. 227717.
93. Vadasz, J., et al. *Vibration Effects on Heat Transfer During Solidification of Paraffin*. in *ASME 2011 International Mechanical Engineering Congress and Exposition*. 2011.
94. Zhou, G., M. Zhu, and Y. Xiang, *Effect of percussion vibration on solidification of supercooled salt hydrate PCM in thermal storage unit.* Renewable Energy, 2018. **126**: p. 537-544.